MECA0023-1

Advanced Solid Mechanics

Project Group 7

Authors :
Devos Valentine (s171149)
Mignolet Maxime (s172404)
Nguyen Dylan (s174507)
Rihon Bryan (s170691)

Professor:
Ponthot Jean-Philippe
Assistant:
Laruelle Cédric

Academic year 2020-2021

Contents

List of Figures

List of Tables

Introduction

Linear elasticity is a concept often studied in the curriculum of a young student in engineering. A material is loaded, deforms, is unloaded and comes back to its initial shape. However, materials' behavior are not limited to this simple model. There is no need to go to a top-notch laboratory to observe that when a spoon is bent, it may remain bent. Materials considered as being in a solid state such as concrete can creep. Actually, there is a wide variety of behaviors that cannot be explained by linear elasticity and, likewise, there is a wide number of models that have sprung up over the decades to try to render these behaviors.

The aim of this project is to study numerically some models linked to elasto-plastic behavior and elasto-viscoplastic behavior. To simplify the problem and have some qualitative insights, the object studied is set to be a simple cube subjected to a surface traction on one of its surfaces, as can be seen in Fig. 1. In this figure, a number has been attributed to each node. Furthermore, the effects of inertial forces and temperature will not be considered to limit the number of parameters varied. The other general hypotheses made throughout this whole project are presented and explained in the next section. The Einstein summation convention holds everywhere.

To begin with, the behavior of an elasto-plastic material is analyzed in Part 1 of this project. Various types of hardening laws are used but all of them are linear. In Part 2, the non-linearity effects of hardening are studied with the same type of material. Afterwards, Part 3 introduces an elasto-viscoplastic material which is studied in the whole section. Finally, the sensibility of the results with respects to the numerical parameters are estimated in Part 4 to ascertain whether or not the results obtained are valid.

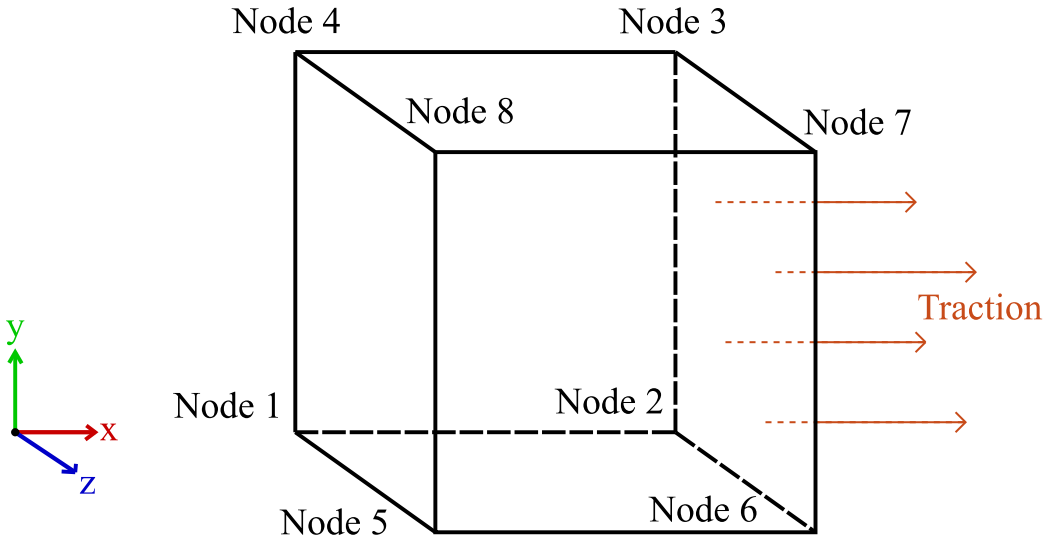

Fig. 1: Representation of the cube subjected to a surface traction in the x direction. The nodes of the cube have been numerated from 1 to 8.

General hypotheses

In this section we present the general hypotheses made in this project. The assumption of small strains is made. It is further assumed that the strain rate D_{ij} may be decomposed additively in an elastic D^{e}_{ij} and a viscoplastic part D^{vp}_{ij}, i.e. $D_{ij} = D^{\mathrm{e}}_{ij} + D^{\mathrm{vp}}_{ij}$. Since we made the small strain assumption, this implies that the strain ε_{ij} is the sum of the elastic strain $\varepsilon^{\mathrm{e}}_{ij}$ and the viscoplastic strain $\varepsilon^{\mathrm{vp}}_{ij}$, i.e. $\varepsilon_{ij} = \varepsilon^{\mathrm{e}}_{ij} + \varepsilon^{\mathrm{vp}}_{ij}$. The existence of a yield function f determining the onset of plasticity is assumed. The extended yield function determine the onset of viscoplasticity. We make the assumption that the plastic flow is given by the associated flow rule. Accordingly to this, the plastic strain rate is given

by $D_{ij}^{\mathrm{p}} = \frac{\partial f}{\partial \sigma_{ij}} / \sqrt{\frac{\partial f}{\partial \sigma_{kl}} \frac{\partial f}{\partial \sigma_{kl}}}$. The same statement can be made in the case of viscoplasticity with the viscoplastic strain rate and the extended yield function.

Studied elasto-plastIic and elasto-viscoplastic models

This section introduces the models studied in this project and the notations associated to them. The models are

- elastic perfectly plastic model,
- isotropic linear hardening,
- kinematic linear hardening,
- mixed linear hardening,
- non-linear kinematic hardening,
- non-linear kinematic hardening mixed with linear isotropic hardening,
- mixed non-linear hardening,
- viscoplasticity with linear isotropic hardening and
- viscoplasticity with linear mixed hardening.

Some of those are studied in a state of plane stress and in a state of plane strain, and some other only in a state of plane stress.

An elastic perfectly plastic solid is a material for which the yield surface remains constant. Consequently, the equivalent von Mises stress $\overline{\sigma}^{\mathrm{VM}} = \sqrt{\frac{3}{2}\sigma_{ij}\sigma_{ij}}$ cannot become larger than the yield stress σ_{y}^0. If it becomes larger, one may interpret it as the failure of the material. This model is used when assuming there is no work hardening[2].

The linear and non-linear isotropic hardening models are models where the yield surface expands isotropically in stress space. This expansion may be linear or non-linear with respect to the equivalent plastic strain $\overline{\varepsilon}^{\mathrm{vp}}$. In the most general case, the yield stress determining the radius of the yield surface is given by:

$$\sigma_{\mathrm{y}} = \sigma_{\mathrm{y}}^0 + h_i(\overline{\varepsilon}^{\mathrm{vp}}), \tag{1}$$

where σ_{y}^0 is the yield stress of the virgin material and h_i is a hardening parameter. In the case of linear hardening, this formula becomes:

$$\sigma_{\mathrm{y}} = \sigma_{\mathrm{y}}^0 + h_i. \tag{2}$$

The non-linear hardening law studied in this project is Voce's saturated law given by:

$$\sigma_{\mathrm{y}} = \sigma_{\mathrm{y}}^{\infty} - \left(\sigma_{\mathrm{y}}^{\infty} - \sigma_{\mathrm{y}}^0\right) \exp\left(-\frac{h_i \overline{\varepsilon}^{\mathrm{vp}}}{\sigma_{\mathrm{y}}^{\infty} - \sigma_{\mathrm{y}}^0}\right), \tag{3}$$

where $\sigma_{\mathrm{y}}^{\infty}$ is another parameter which can be seen as the saturated yield stress. The main advantage of that model lies in its simplicity. The isotropicity of the expansion makes the analytical computations a lot easier. However it cannot represent Bauschinger effect. This is a real drawback when studying loading/unloading cycles, as it is done in this project.

In the linear and non-linear kinematic models, there is no expansion of the yield surface. The surface translates in the stress space. The translation tensor is denoted $\boldsymbol{\alpha}$ and is called the backstress tensor. In the linear case, the evolution of the backstress tensor is prescribed by:

$$\dot{\boldsymbol{\alpha}} = \frac{2}{3} h_k \boldsymbol{D}^{\mathrm{vp}}, \tag{4}$$

where h_k is a hardening parameter. Whereas, for the non-linear case we use Armstrong Frederick's evolution law:

$$\dot{\boldsymbol{\alpha}} = \frac{2}{3} h_k \boldsymbol{D}^{\text{vp}} - \eta_k \dot{\bar{\varepsilon}}^{\text{vp}} \boldsymbol{\alpha}, \tag{5}$$

where η_k is yet another parameter. The term that contains this parameter represents dynamic recovery which is the phenomenon in which the backstress tends to return to its original position. The material is said to have a dynamic fading memory.

In the case of mixed hardening, an isotropic and a kinematic hardening law are put together so that both the yield stress and the backstress evolve. Hence, the yield surface has both a varying size and a varying center position. To combine the two hardening, a weighting parameter θ is defined such that

$$\Big\{ h_i \; = \; \theta h, h_k \; = \; (1-\theta)h, \tag{6}$$

with $h = h_i + h_k$. For this project, the value of theta used is set to $\theta = 0.2$.

The viscoplasticity is modelled using Perzyna's law. Perzyna law states that

$$\lambda = \sqrt{\frac{3}{2}} \left\langle \frac{\overline{\sigma}^{\text{VM}} - \sigma_{\text{y}}}{\eta} \right\rangle = \sqrt{\frac{3}{2}} \left\langle \frac{f}{\eta} \right\rangle, \tag{7}$$

where $\langle \cdot \rangle$ are Mc Auley brackets, i.e.

$$\langle x \rangle = \begin{cases} x & \text{if } x \geq 0, \\ 0 & \text{if } x < 0. \end{cases} \tag{8}$$

The parameter η is a viscosity parameter. We see that the von Mises stress $\overline{\sigma}^{\text{VM}}$ may become larger than the yield stress, which wasn't allowed with all the previous models. We can say that viscosity allows for some overstress. In part 3, a reformulation of Perzyna's law as a yield criterion with the help of an *extended* yield function shall be explained in Part 3.

1 Part 1: Study of elasto-plastic behavior with linear hardening

The first material behavior considered is the elasto-plastic one with linear hardening. The cube is subjected to several loading/unloading cycles where the surface traction evolves linearly from 0 to a set value t_{max}, then linearly to $-t_{\text{max}}$ and finally back to 0.

In order to determine the maximal surface traction t_{max} needed in a loading cycle to attain a permanent equivalent viscoplastic deformation $\overline{\varepsilon}^{\text{vp}}{}_{\text{max}}$ with isotropic hardening, the theoretical results are used to guide the numerical simulation. We recall that an elasto-plastic material is rate independent. Therefore, the period of the loading cycle should not impact t_{max}. For a linear isotropic hardening model, t_{max} takes the analytical expression: $t_{\text{max}} = \sigma_{\text{y}}^0 + h\overline{\varepsilon}^{\text{vp}}{}_{\text{max}}$. Replacing with the numerical values ($\sigma_{\text{y}}^0 = 200$ [MPa], $h = 30$ [GPa], $\overline{\varepsilon}^{\text{vp}}{}_{\text{max}} = 0.35\%$ [-]), we get $t_{\text{max}} = 305$ [MPa]. When running Metafor with this value, the permanent equivalent viscoplastic deformation is exactly equal to the sought value.

We shall now study the behavior of the cube, considering different models, in both a state of plane stress and a state of plane strain. The considered models are :

- the perfectly plastic model,
- the linear isotropic hardening,
- the linear kinematic hardening
- and the linear mixed hardening.

The study is structured in two main sections, one for the state of plane stress and the other for the state of plane strain. Inside both section, one sub-section is dedicated to each model in which we analyze the behavior of the cube. In order to compare the different model, the relevant variables to study the behavior of the cube are all extracted from node 7 and express in the Haigh Westergaard's space. The tensorial variables are thus diagonal and then easier to compare with other models.

1.1 Case of the state of plane stress

The state of plane is a special case where a 3D behavior can be simplified into a 2D one and enables thus to observe analysis in 2D frame. In the case of plane stress state, the stress component associated to one axis are null. In our case, the stress components are null along two axes (y and z axes). This further simplifies the problem.

1.1.1 Perfectly plastic model

When in a state of plane stress, the perfectly plastic model fails. The yield function becomes positive when $|p(t)| > \sigma_{\text{y}}^0$. In no case, can the yield function take positive values. This indicates the failure of the model to represent reality.

1.1.2 Linear isotropic hardening

In the perfectly plastic model, the yield surface is assumed not to change with stress history. However, as many materials harden during plastic deformation, the stress required to induce further plastic deformation increases. Consequently the yield surface must be modified. As the hardening is referred to as isotropic, the expansion of the yield surface is uniform in all directions in the stress space. The yield function has thus the form,

$$f\left(\sigma_{ij}, \sigma_{\text{y}}^0 + h_i\overline{\varepsilon}^{\text{p}}\right) = \overline{\sigma}^{\text{VM}} - \sigma_y^0 + h_i(\overline{\overline{\varepsilon}^{\text{p}}}) = 0. \tag{9}$$

In order to describe the new radius $\sigma_{\mathrm{y}} = \sigma_y^0 + h_i \bar{\varepsilon}^{\mathrm{p}}$ of the yield surface, the equivalent plastic deformation $\bar{\varepsilon}^{\mathrm{p}}$ is generally used. It is then an important variable to observe during simulations.

The cube was subjected to 3 loading/unloading cycles with a maximal applied load equal to $t_{\max}$. The results are represented on Fig. 2. We observe that, once the applied load reaches its maximum value, the equivalent plastic strain remains constant and the yield stress attains its maximum value. This indicates that no more plastic deformation occurs. The cube deforms only elastically. Once the cube has been plastically deformed, we observe that even when the imposed load is zero the strains are non-zero. We may say that the cube has been irreversibly deformed. The cube has been elongated in the x direction ($\varepsilon_{xx} > 0$) and compressed in the y and z directions ($\varepsilon_{yy} = \varepsilon_{zz} > 0$).

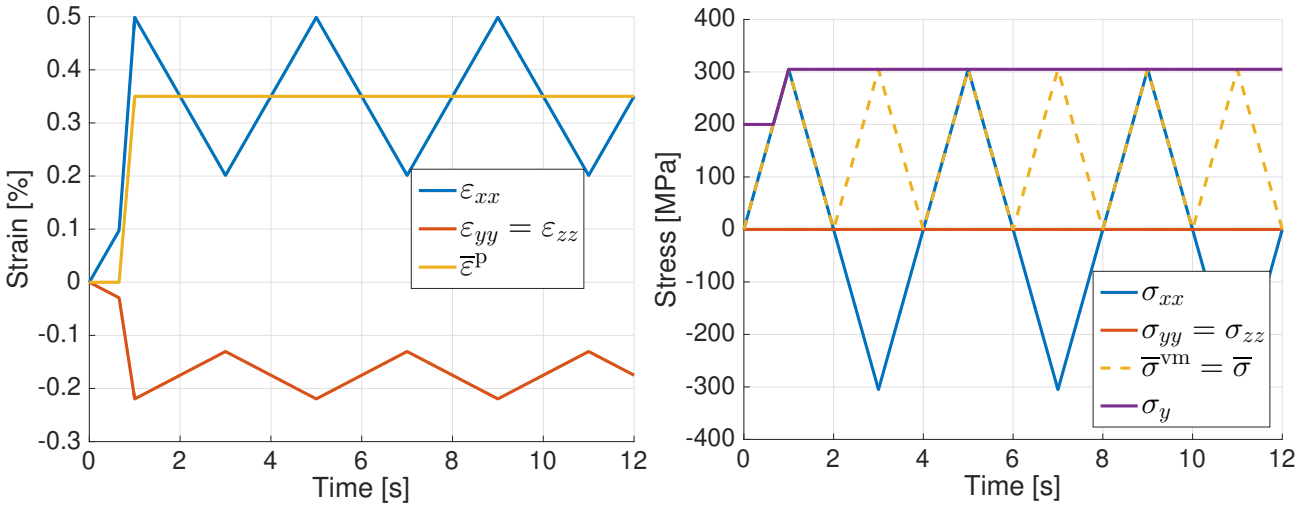

(a) Strain (b) Stress

Fig. 2: Linear isotropic hardening behavior over time when subjected to 3 loading/unloading cycles in plane stress with a maximal loading equal to $t_{\max}$.

A second observation is that some variables like the equivalent plastic deformation or the yield stress reach their final value on the first loading and remain constant after that. The other variables are harmonic after the first cycle. As said in the beginning of this part, a 0.35% of permanent equivalent plastic deformation is met again for this load.

For a "normal" cycle, the cube is first subjected to traction and then to compression. To know if this order has an impact, an inverse cycle can be considered. The results obtained can be observed in Fig. 3.

1.1.3 Linear Kinematic hardening

Another model to represent hardening is the kinematic hardening model which assumes that the yield surface keeps its initial shape and size but translates in the stress space during plastic deformation. The backstress tensor $\boldsymbol{\alpha}$ describes the position of the center of the yield surface.

As for isotropic hardening, a first simulation is run with a maximal load of 305 MPa and 3 loading/unloading cycles. The results are shown on Fig. 4. Contrary to isotropic hardening, the equivalent plastic deformation does not reach a maximum value at the end of the first loading but increases at each loading (in traction and in compression). It can be said that the final value reached by the equivalent plastic deformation depends on the number of cycles. Beside this, the increment of equivalent plastic deformation during the first loading is smaller than during the other loading or unloading. This can be explained by the fact that the yield surface center does not come back at the origin after one cycle. The equivalent backstress is non-zero after one cycle.

From Fig. 4a, it can also be observed that the value reached by the equivalent plastic strain after the first loading is equal to 0.35% as it is obtained with isotropic hardening. Contrary to isotropic

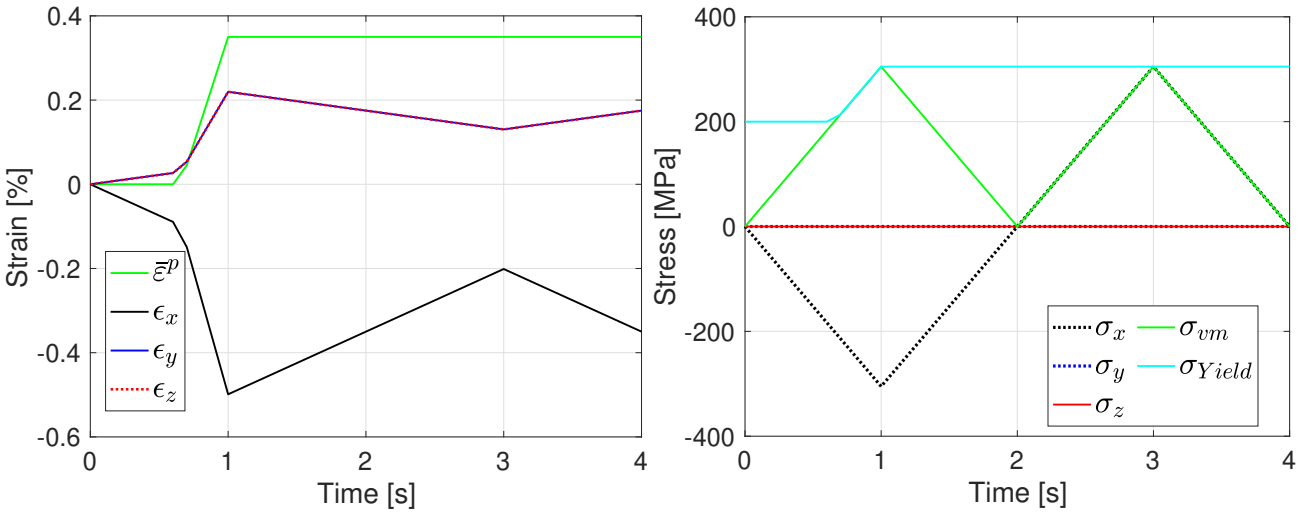

(a) Strain (b) Stress

Fig. 3: Linear isotropic hardening behavior over time for a reversed load with $t_{\max} = 305$ MPa and 1 loading/unloading cycle in plane stress.

hardening, the strains have a zero time average value. However at the end of a cycle, the strains are non-zero.

As for isotropic hardening, a simulation is run with a reverse cycle to observe if it have an impact on the results which are presented in Fig. 5.

1.1.4 Linear mixed hardening

The two previous hardening models have very different behaviors. Indeed the yield surface evolution are completely different. However it is possible to combine them to form a new hardening model with a more complex evolution of the yield surface and which is a priori more realistic and models more accurately actual materials. However, one more hardening parameter is required to construct this model.

As done before, a simulation is firstly run with a load of 305 Mpa and 3 loading/unloading cycles and the results are presented in Fig. 6. We observe that, as in the case of kinematic hardening, the equivalent plastic strain do not stop increasing after the first loading. However, it tends towards a finite value instead of increasing indefinitely. This means that the cube deforms less and less plastically and that after a infinite amount of cycles the cube no more deforms plastically and all the deformations over a cycle are elastic. The yield stress tends towards $t_{\max}$ and the equivalent backstress tends towards zero. This can be interpreted as the radius of the yield surface becoming larger and therefore the yield surface center doesn't need to translate as much it did during the last loadings in order to satisfy the yield criterion.

It can also be observed that the value reached by the equivalent plastic strain after the first loading is equal to 0.35% as it is obtained with isotropic hardening. The diagonal elements of the strain tensor tend towards zero as the number of cycle increases. This suggests that after an infinite amount of cycles, the cube retrieves its initial shape.

For the same reason that it have been done for the previous model, Fig. 3 sows the results for a reverse cycle.

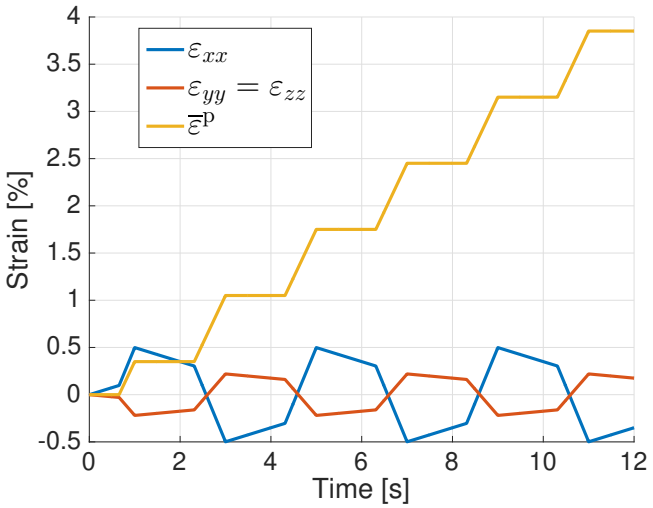

(a) Strain

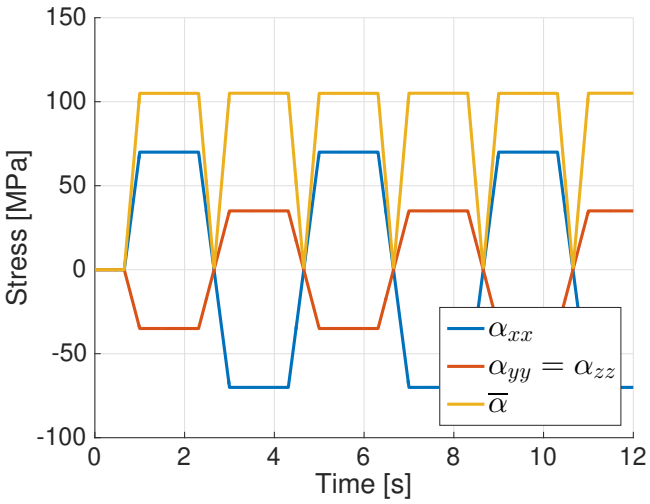

(b) Back-stress

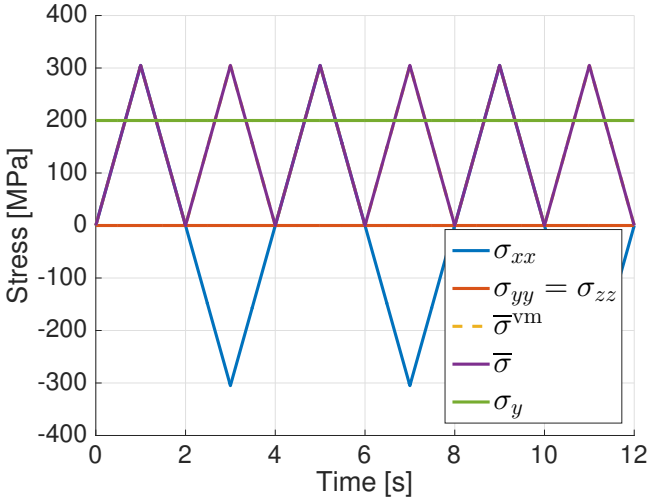

(c) Stress

Fig. 4: Linear kinematic hardening behavior for 3 loading/unloading cycles with a maximal load equal to $t_{\max}$ in plane stress.

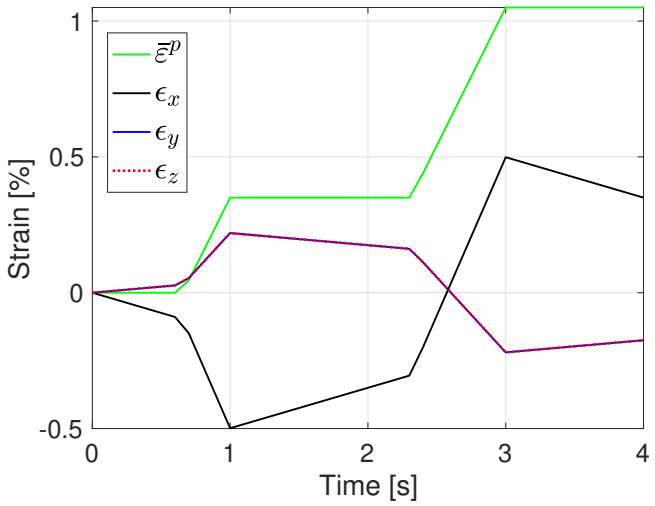

(a) Strain

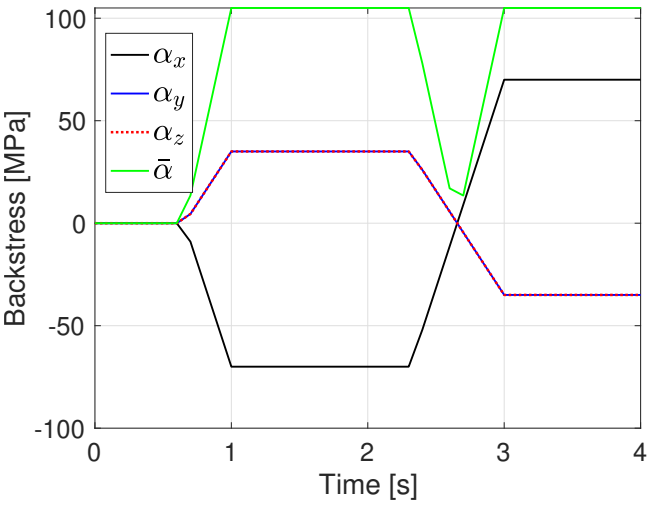

(b) Back-stress

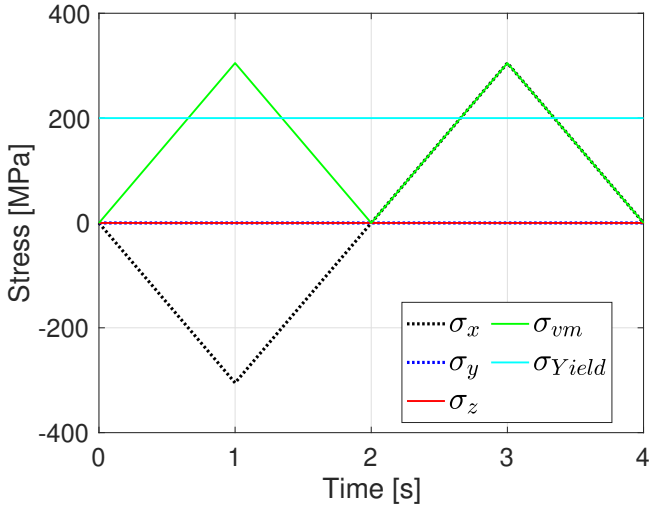

(c) Stress

Fig. 5: Linear kinematic hardening behavior for a reverse load with $t_{\max} = 305$ MPa and loading/unloading cycle in plane stress.

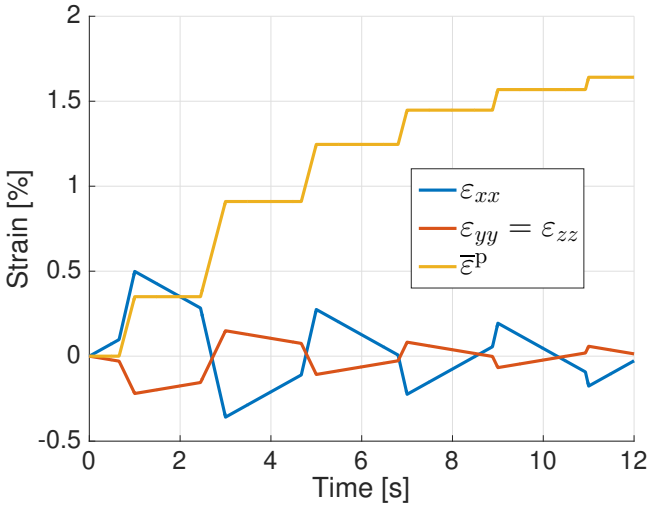

(a) Strain

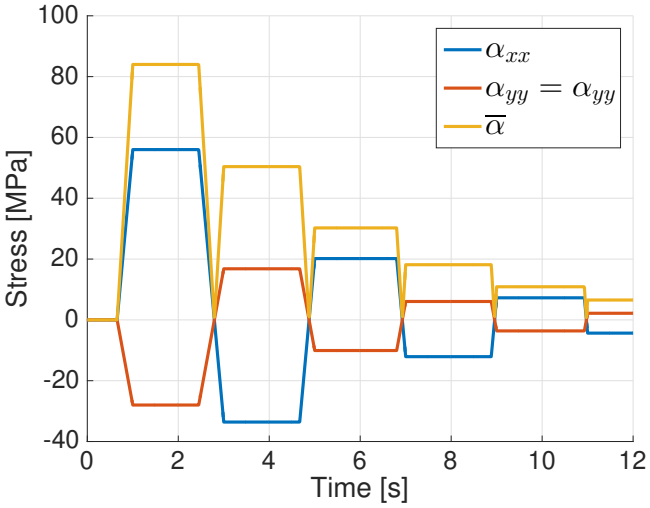

(b) Backstress

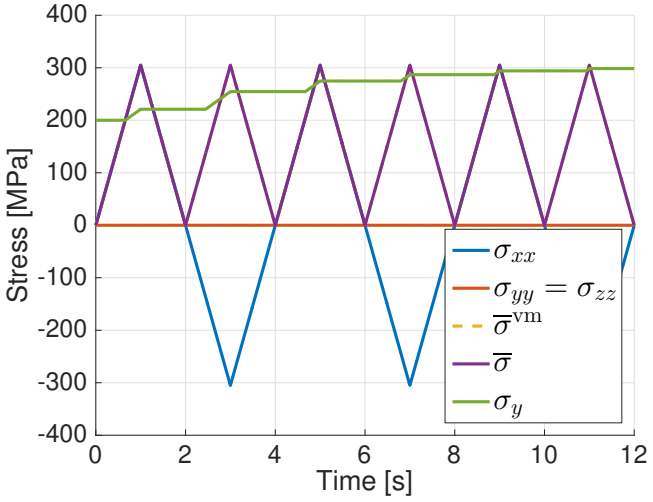

(c) Stress

Fig. 6: Mixed hardening behavior for $t_{\max} = 305$ MPa and 3 loading/unloading cycles in plane stress.

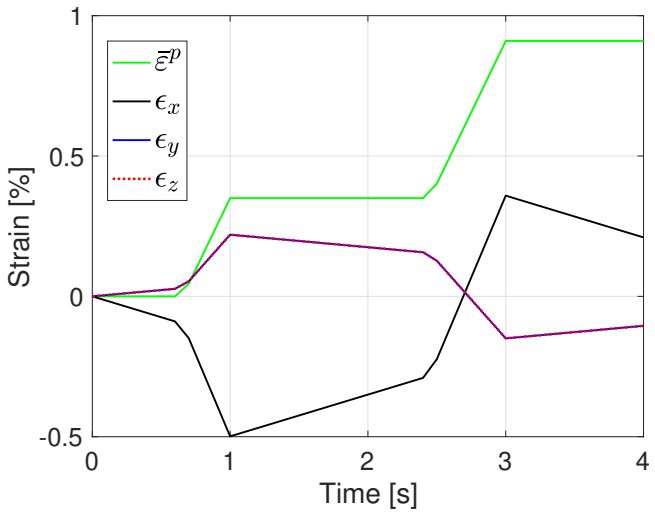

(a) Strain

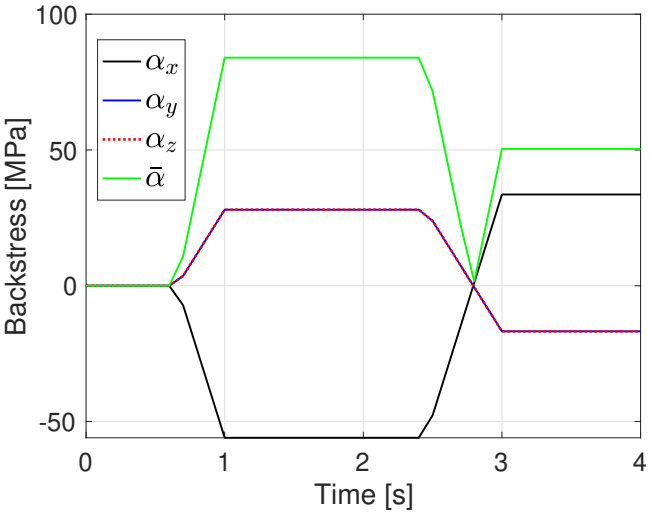

(b) Backstress

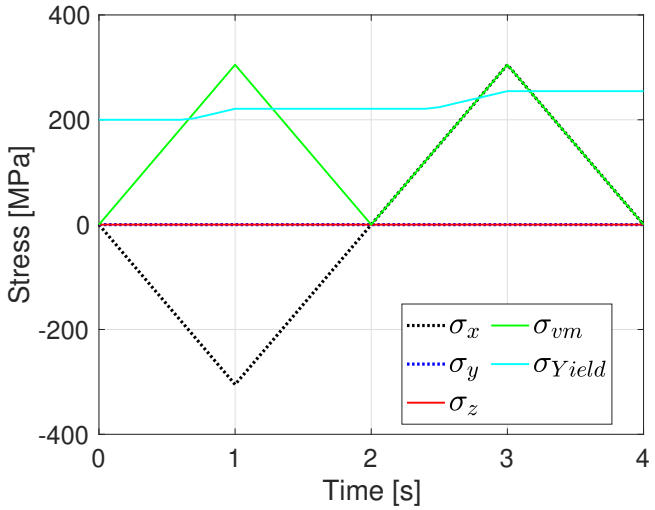

(c) Stress

Fig. 7: Mixed hardening behavior for a reverse loading with $t_{\max} = 305$ MPa and 1 loading/unloading cycle in plane stress.

1.2 Case of the state of plane strain

Another special case that reduces the model analysis into 2D is the state of plane strain. The deformation along one axis must be cancelled. We choose to cancel the deformations along the z-axis. Using the strain-displacement relations, we must require:

$$\varepsilon_{xz} = \frac{1}{2}\left(\frac{\partial u_x}{\partial z} + \frac{\partial u_z}{\partial x}\right) = 0, \tag{10}$$

$$\varepsilon_{yz} = \frac{1}{2}\left(\frac{\partial u_y}{\partial z} + \frac{\partial u_z}{\partial y}\right) = 0, \tag{11}$$

$$\varepsilon_{zz} = \frac{\partial u_z}{\partial z} = 0, \tag{12}$$

where u_i is the displacement field. In order to insure this, some additional boundary conditions on the displacements must be added. Since we want to cancel the deformations along the z-axis, it seems intuitive to block the displacement along the z-axis for the two sides normal to the z-axis. Then the displacement along the z-axis is null everywhere in the cube. The nullity of the deformations reduces itself to the independence of the displacement field with respect to the z coordinate. Intuitively, we may say that this is the case since the boundary conditions, the applied loading and the geometry are independent of z. The problem is even invariant under reflection perpendicular to the z-axis. When running metafor with the additional boundary condition, we observe a state of plane strain.

1.2.1 Perfectly plastic model

When a simulation is run with the perfectly plastic model in plane strain, it suddenly stop as the plastic deformation starts. This is due to the yield function turning positive. In no case, this is physically acceptable. As for the state of plane stress, this indicates the failure of the model to represent the reality.

1.2.2 Linear isotropic hardening

In order to compare with other models and particularly with the same hardening model as in plane stress, Fig. 8 shows the results of a simulation with a linear isotropic hardening behavior for $t_{\text{max}} = 305$ MPa and 3 loading/unloading cycles in plane strain.

First, we can observe on Fig. 8a that the deformation along the z-axis is null as expected for plane strain. Moreover, the final value reached by the equivalent plastic deformation is smaller than that one obtained in plane stress. This is due to the fact that a larger fraction of the applied loading is lost in hydrostatic pressure. Indeed, we know, thanks to Bridgman's experiments, that the hydrostatic pressure does not generate plasticity. Only the deviatoric part of the stress tensor can generate plasticity. A strange phenomenon to which we didn't fin any explanation is the staircase formed by $\bar{\varepsilon}^{\text{p}}$ and by σ_y.

Here again, the results for a reverse cycle are present in Fig. 9

1.2.3 Linear kinematic hardening

As for the plane stress, the Fig. 10 shows the results of a simulation with a linear kinematic hardening behavior for $t_{\text{max}} = 305$ MPa and 3 loading/unloading cycles in plane strain. Also for this model, the equivalent plastic deformation is smaller in plane strain than in plane stress. It is certainly due to the fact that a stress appears along the z-axis because the displacement is fixed for this direction. This the same for the backstress.

In another hand, Fig. 11 contains the results of a simulation with a reverse cycle and the same load as the previous one to observe an potential change in the behaviour for some variable.

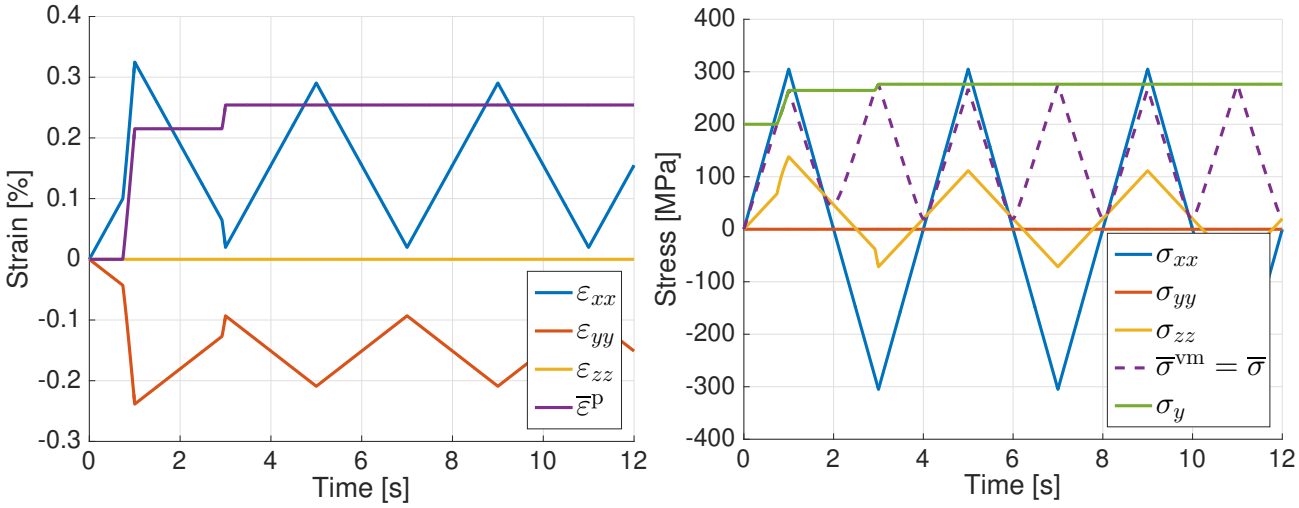

(a) Strain

(b) Stress

Fig. 8: Linear isotropic hardening behavior for $t_{\max} = 305$ MPa and 3 loading/unloading cycle in plane strain.

1.2.4 Linear mixed hardening

One last time, we run a simulation with a mixed hardening model with a load of $t_{\max} = 305$ for 3 cycles but this time with plane strain conditions. Fig.12 shows then the relevant variables behaviour that can be analysis. By observing these graphs, the same assessments are recovered as the two previous model in plane strain. It is in a way logical since the mixed hardening model is a combination of the isotropic model and the kinematic model.

It is also a last case where we can run a simulation for a reverse cycle and observe if something change. That's why Fig. 13 contains the results obtained in order to compare with previous ones.

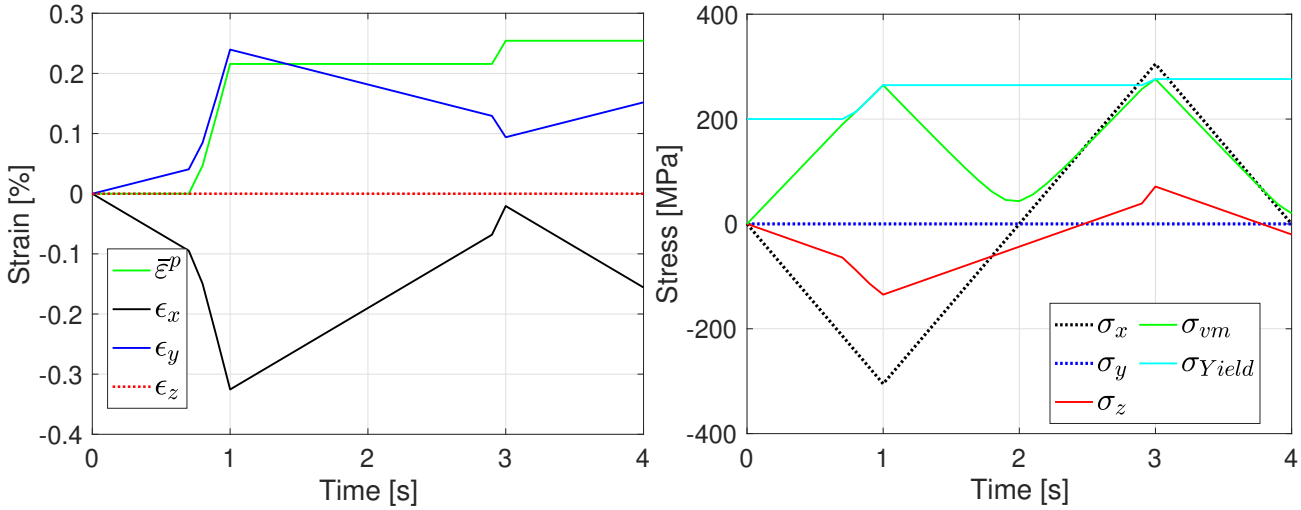

(a) Strain (b) Stress

Fig. 9: Linear isotropic hardening behavior for a reverse cycle with $t_{\max} = 305$ MPa and 1 loading/unloading cycle in plane strain.

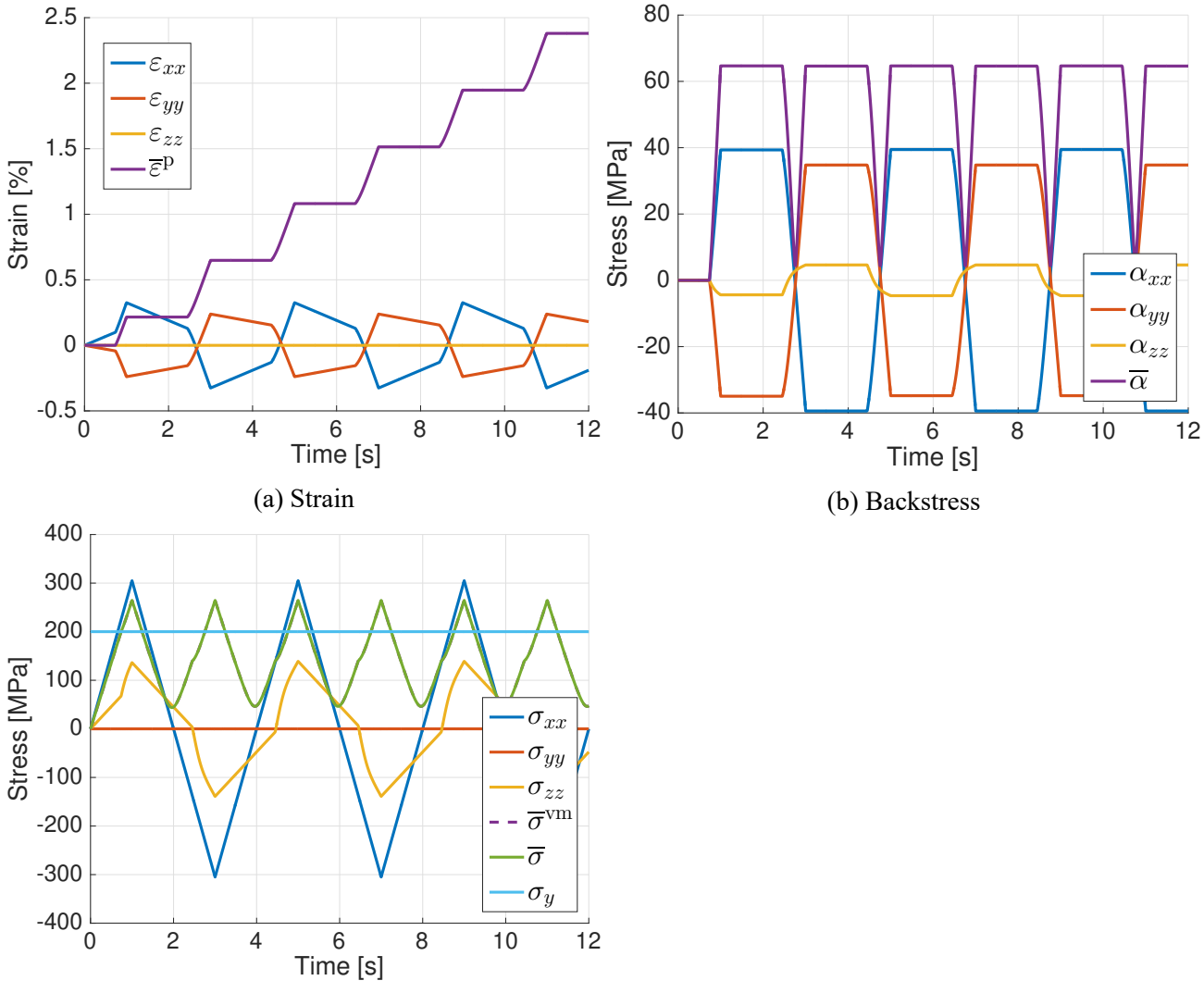

(a) Strain (b) Backstress

(c) Stress

Fig. 10: Linear kinematic hardening behavior for $t_{\max} = 305$ MPa and 3 loading/unloading cycles in plane strain.

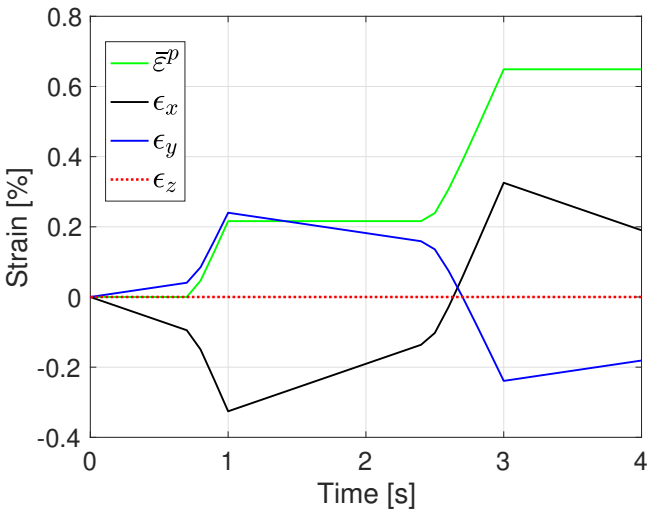

(a) Strain

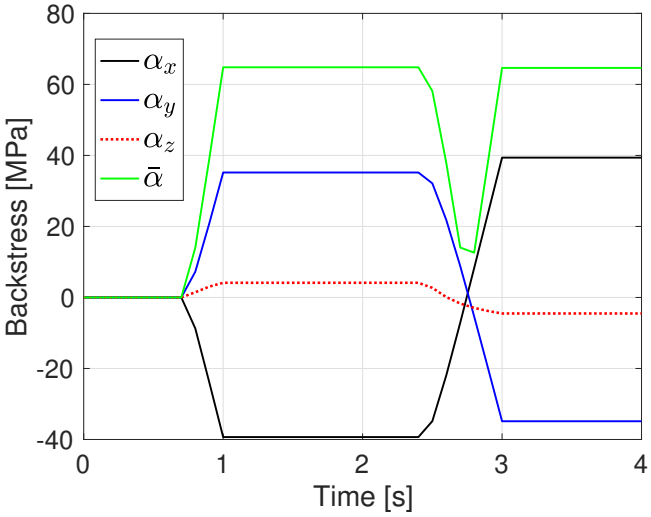

(b) Backstress

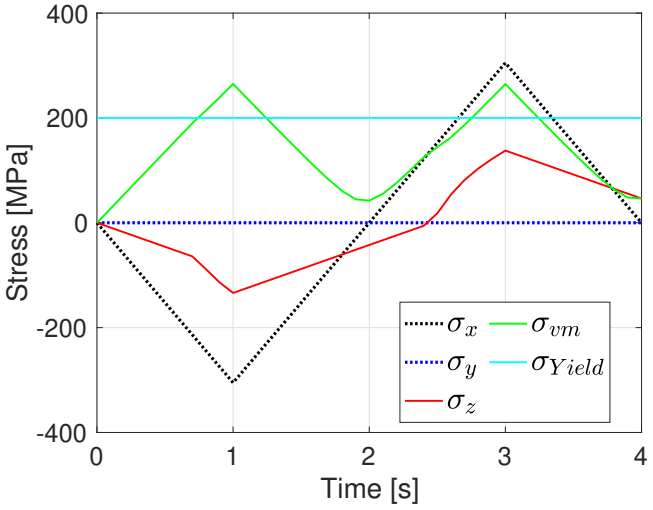

(c) Stress

Fig. 11: Linear kinematic hardening behavior for a reverse loading cycle with $t_{\max} = 305$ MPa and 1 loading/unloading cycle in plane strain.

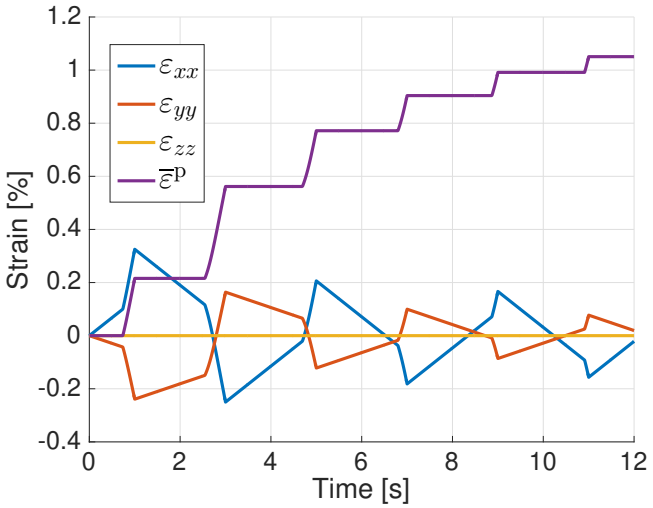

(a) Strain

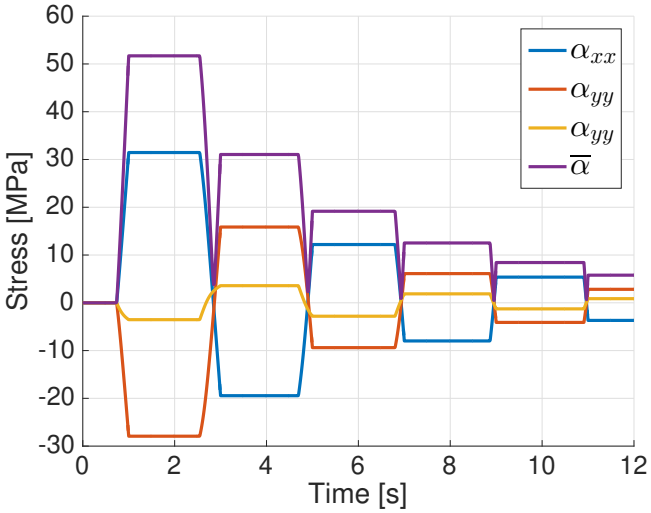

(b) Backstress

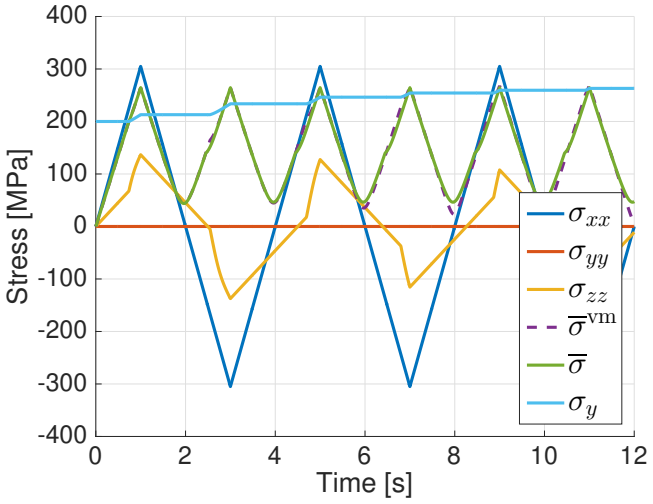

(c) Stress

Fig. 12: Linear mixed hardening behavior for $t_{\max} = 305$ MPa and 3 loading/unloading cycles in plane strain.

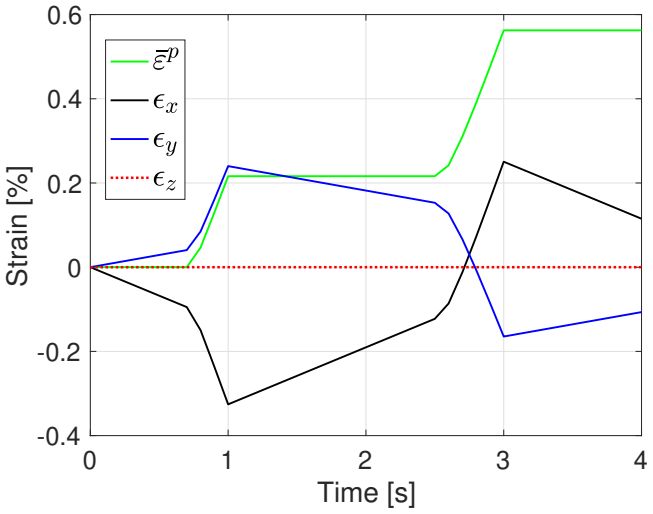

(a) Strain

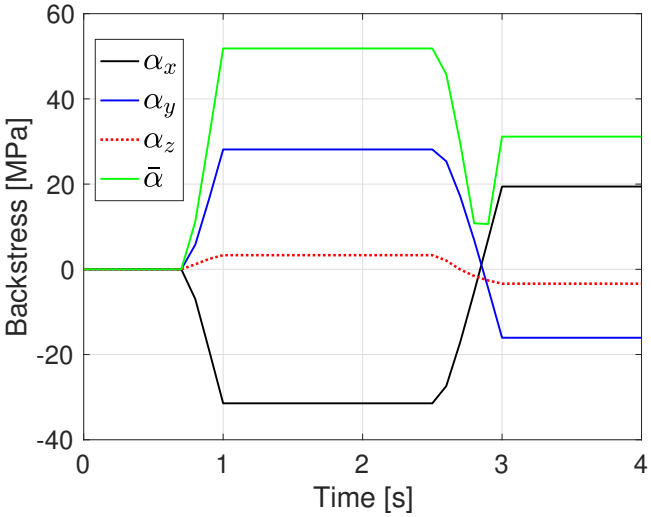

(b) Backstress

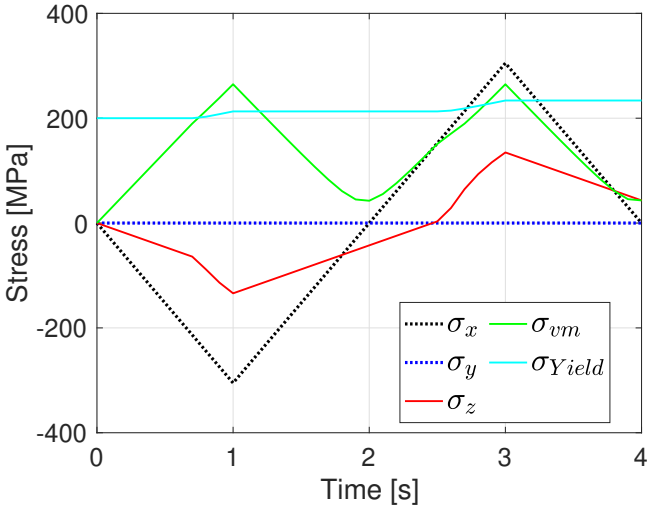

(c) Stress

Fig. 13: Linear mixed hardening behavior for a reverse cycle with $t_{\max} = 305$ MPa in plane strain.

1.3 General analysis

1.3.1 Equivalent stress and equivalent backstress

The first thing to say is that it is obvious that the equivalent backstress $\bar{\alpha}$ take a zero value for a isotropic hardening model when the load evolves from t_{max} to $-t_{\text{max}}$ as the notion of backstress is not relevant in the isotropic model and then equal zero during the whole process. However, for the others models of hardening and in both state of plane, the equivalent backstress takes a zero value when the load goes from t_{max} to $-t_{\text{max}}$.

Concerning the equivalent stress, we can observed in the different stress graphs that it takes a zero value when the load evolves from t_{max} to $-t_{\text{max}}$ regardless of the linear hardening model or the plane state considered. Moreover, when the load is zero at the end of the cycles, the equivalent stress take a zero value in all cases, except in the case of linear kinematic and mixed hardening in plane strain where it is slightly out of phase and a zero value just before the end of the last cycles.

1.3.2 Equivalent plastic strain

No matter the linear hardening model considered, we observe that the equivalent plastic strain takes the same value (which may differ if we consider a state of plane stress or plane strain). Let us try to explain this phenomenon. We start by writing the consistency equation:

$$\dot{f} = \frac{\partial f}{\partial \sigma_{ij}}\dot{\sigma}_{ij} - \frac{\partial f}{\partial \sigma_{ij}}\dot{\alpha}_{ij} - \dot{\sigma}_y = 0. \tag{13}$$

Further developments lead to:

$$\begin{aligned}\frac{\partial f}{\partial \sigma_{ij}}\dot{\sigma}_{ij} &= \sqrt{\frac{3}{2}}N_{ij}\frac{2}{3}h_k D_{ij}^{\text{vp}} + h_i\dot{\bar{\varepsilon}}^{\text{p}} \\ &= \sqrt{\frac{2}{3}}h_k\lambda N_{ij}N_{ij} + \sqrt{\frac{2}{3}}h_i\lambda \\ &= \sqrt{\frac{2}{3}}h\lambda. \end{aligned} \tag{14}$$

Knowing that the loading is a piecewise linear function, we have that $\frac{\partial f}{\partial \sigma_{ij}}\dot{\sigma}_{ij}$ is piecewise constant. But most importantly it is independent of the linear hardening model considered and therefore λ is also independent of the linear hardening model. By definition, we have $\dot{\bar{\varepsilon}}^{\text{vp}} = \sqrt{\frac{2}{3}}\lambda$. The time of first entrance in the plastic domain and the time when the unloading starts (i.e. when the loading is equal to t_{max}) don't depend on the hardening model. Therefore, the value of $\bar{\varepsilon}^{\text{vp}}$ when the loading reaches its maximum value, is also independent of the model considered.

The loading increasing from zero to t_{max} can be seen as the imposed loading during a tensile test. Therefore, we can interpret this accordance between the three linear hardening as the fact that during a tensile test they should give the same results.

1.3.3 Reverse loading

In this section, we analyse if there are any significant difference between a normal cycle and a reverse cycle, i.e. if the fact that the cube is, first, put in traction and then in compression has an influence. The figures representing the reverse cycles are Fig. 3, 5, 7, 9, 11, 13. We chose to keep those figures next to their counterpart and didn't regroup all of them in this section, in order to make comparisons between normal and reverse cycle easier.

On Fig. 3 (linear isotropic hardening in a state of plane stress), we see that the strains have flipped sign in comparison to the normal cycle (Fig. 2). This means that, when the loading is removed,

the cube shall be compressed along the x direction and elongated in the y and z directions. The same conclusion can be drawn when dealing with a state of plane strain. When considering the two other models this sign flip has no influence on the deformations once the load is removed. However the backstress tensor is influenced since it doesn't get back to zero when removing the loading. All the components of the backstress tensor flip sign. This may have a strong influence on the future behavior of the cube since the backstress induces anisotropy. And we see that this anisotropy may be in one direction or the other depending on the fact that the last plastic deformation was performed in compression or in traction. If the last plastic deformation was performed in traction, the cube will deform more easily in traction than in compression. The cube will enter more rapidly the plastic region in compression than in traction.

1.3.4 Plastic dissipation

The last quantity to analyze for these models is the plastic dissipation $\mathbb{D}$ which represents an irreversible work which generates heat or atomic lattices rearrangements when the material is deforming in the plastic domain. It is defined as follows:

$$\mathbb{D} \;=\; \sigma_{ij}\, D_{ij}^{\text{vp}} \;=\; \sigma_{ij}\dot{\varepsilon}_{ij}^{\text{vp}}. \tag{15}$$

Let us develop this formula while remaining in the general case:

$$\mathbb{D} = \lambda \sigma_{ij} N_{ij}. \tag{16}$$

From Eq. (14), we have the expression of the λ. We can insert it in $\mathbb{D}$ and we obtain:

$$\mathbb{D} = \sqrt{\frac{3}{2}}\frac{1}{h}\frac{\partial f}{\partial \sigma_{ij}}\dot{\sigma}_{ij}\sigma_{kl}N_{kl} = \frac{3}{2}\frac{1}{h}\dot{\sigma}_{ij}N_{ij}\sigma_{kl}N_{kl} \tag{17}$$

During the loading, $\dot{\sigma}_{ij}$ and N_{ij} are constant and the components of the stress tensor σ_{ij} increase (in absolute value) linearly with time. Hence, $\mathbb{D}$ also increases linearly with time. This result is independent of the linear model considered. The difference in the dissipated energy between them lies in the fact that they don't spend the same amount of time in the plastic region.

2 Part 2: Study of elasto-plastic behavior with non-linear hardening

All the models that have hitherto been seen used linear hardening. In this section, the non-linear effects of the kinematic hardening law described by Armstrong Frederick's evolution law of the backstress tensor are studied. The cube remains elasto-plastic with the same material parameters and is set in a plane stress state.

2.1 The dynamic recovery and its parameter η_k

First of all, the influence of the dynamic recovery parameter η_k is studied in the case of a simple kinematic non-linear hardening and the case of a mixed hardening, where the kinematic law is non-linear.

The first thing to notice is that η_k is adimensional so that it satisfies the dimensional units contained within the evolution law of the backstress tensor, which is rewritten as follows:

$$\dot{\alpha}_{ij} \;=\; \frac{2}{3} h_k D^{\mathrm{p}}_{ij} \;-\; \eta_k \dot{\bar{\varepsilon}}^{\mathrm{p}} \alpha_{ij}. \tag{18}$$

If the hardening is mixed, then the yield stress follows the law that were described by Eq. 2 and Eq. 3

These two equations in addition to Eq. 18 can be rewritten in the general form

$$\dot{\boldsymbol{q}}^{(k)} \;=\; \lambda \times r^{(k)}(\boldsymbol{\sigma}, \boldsymbol{q}), \tag{19}$$

knowing that $D^{\mathrm{p}}_{ij} = \lambda N_{ij}$ and $\dot{\bar{\varepsilon}}^{\mathrm{p}}_{ij} = \sqrt{\frac{2}{3}}\lambda$, where λ is the plastic flow intensity and N_{ij} is the plastic flow direction:

$$\dot{\alpha}_{ij} \;=\; \lambda \left(\frac{2}{3} h_k N_{ij} \;-\; \sqrt{\frac{2}{3}} \eta_k \alpha_{ij} \right), \tag{20}$$

$$\dot{\sigma}_{\mathrm{y}} \;=\; \begin{cases} \lambda \left(\sqrt{\dfrac{2}{3}} h_i \right) & \text{for the isotropic linear hardening,} \qquad (21) \\ \lambda \left(\sqrt{\dfrac{2}{3}} h_i \exp\left(-\dfrac{h_i}{\sigma_y^{\infty} - \sigma_y^0} \bar{\varepsilon}^{\mathrm{p}} \right) \right) & \text{for the isotropic non-linear hardening.} \qquad (22) \end{cases}$$

Then, in the case of nonlinear mixed hardening, the generalized plastic modulus H^{p} is defined as

$$H^{\mathrm{p}} \;=\; -\frac{\partial f}{\partial \boldsymbol{q}^{(k)}} * r^{(k)}(\boldsymbol{\sigma}, \boldsymbol{q}), \tag{23}$$

so that the consistency condition can be written as follows:

$$\begin{aligned} 0 \;=\; \dot{f} \;&=\; \frac{\partial f}{\partial \sigma_{ij}} \dot{\sigma}_{ij} \;+\; \frac{\partial f}{\partial \boldsymbol{q}^{(k)}} * \dot{\boldsymbol{q}}^{(k)} \\ &=\; \frac{\partial f}{\partial \sigma_{ij}} \dot{\sigma}_{ij} \;+\; \frac{\partial f}{\partial \boldsymbol{q}^{(k)}} * \left(\lambda \, r^{(k)}(\boldsymbol{\sigma}, \boldsymbol{q}) \right) \\ &=\; \frac{\partial f}{\partial \sigma_{ij}} \dot{\sigma}_{ij} \;-\; \lambda \, H^{\mathrm{p}}. \end{aligned} \tag{24}$$

So, the generalized plastic modulus H^{p} can be rewritten as

$$H^{\mathrm{p}} \;=\; \frac{1}{\lambda} \frac{\partial f}{\partial \sigma_{ij}} \dot{\sigma}_{ij}. \tag{25}$$

The expression can be further developed, knowing that, using the Von Mises yield criterion, the derivative can be written as

$$\frac{\partial f}{\partial \sigma_{ij}} \;=\; \frac{\partial f}{\partial s_{ij}} \;=\; \sqrt{\frac{3}{2}}\frac{s_{ij}-\alpha_{ij}}{\sqrt{(s_{kl}-\alpha_{kl})(s_{kl}-\alpha_{kl})}} \;=\; -\frac{\partial f}{\partial \alpha_{ij}} \;=\; N_{ij}\sqrt{\frac{3}{2}}. \tag{26}$$

In the case of nonlinear mixed hardening, the consistency condition is rewritten as follows:

$$\begin{aligned} 0 \;&=\; \frac{\partial f}{\partial \sigma_{ij}}\dot{\sigma}_{ij} \;+\; \frac{\partial f}{\partial \alpha_{ij}}\dot{\alpha_{ij}} \;+\; \frac{\partial f}{\partial \sigma_y}\dot{\sigma_{\mathrm{y}}} \\ &=\; \frac{\partial f}{\partial \sigma_{ij}}\dot{\sigma}_{ij} \;-\; \frac{\partial f}{\partial \sigma_{ij}}\dot{\alpha_{ij}} \;-\; \dot{\sigma_{\mathrm{y}}} \\ \Leftrightarrow \quad \frac{\partial f}{\partial \sigma_{ij}}\dot{\sigma}_{ij} \;&=\; \frac{\partial f}{\partial \sigma_{ij}}\dot{\alpha_{ij}} \;+\; \dot{\sigma_{\mathrm{y}}}. \end{aligned} \tag{27}$$

Replacing $\dot{\alpha_{ij}}$ and $\dot{\sigma_{\mathrm{y}}}$ with their expressions yields:

$$\frac{\partial f}{\partial \sigma_{ij}}\dot{\sigma}_{ij} \;=\; \lambda\left[\frac{\partial f}{\partial \sigma_{ij}}\left(\frac{2}{3}h_k N_{ij} - \eta_k\sqrt{\frac{2}{3}}\alpha_{ij}\right) \;+\; \sqrt{\frac{2}{3}}h_i(\bar{\varepsilon}^{\mathrm{p}})\right]. \tag{28}$$

Inserting equation (26), we get:

$$H^{\mathrm{p}} \;=\; \frac{1}{\lambda}\frac{\partial f}{\partial \sigma_{ij}}\dot{\sigma}_{ij} \;=\; \sqrt{\frac{2}{3}}h_i(\bar{\varepsilon}^{\mathrm{p}}) \;+\; \sqrt{\frac{2}{3}}h_k - \eta_k\frac{(s_{ij}-\alpha_{ij})\alpha_{ij}}{\sqrt{(s_{kl}-\alpha_{kl})(s_{kl}-\alpha_{kl})}}. \tag{29}$$

Particularizing for linear isotropic hardening, the generalized plastic modulus takes the form:

$$H^{\mathrm{p}} \;=\; \sqrt{\frac{2}{3}}h - \eta_k\frac{(s_{ij}-\alpha_{ij})\alpha_{ij}}{\sqrt{(s_{kl}-\alpha_{kl})(s_{kl}-\alpha_{kl})}} \tag{30}$$

and for non-linear isotropic hardening:

$$H^{\mathrm{p}} \;=\; \sqrt{\frac{2}{3}}\left[h_i\exp\left(-\frac{h_i\bar{\varepsilon}^{\mathrm{p}}}{\sigma_u^{\infty}-\sigma_y^0}\right)+h_k\right] - \eta_k\frac{(s_{ij}-\alpha_{ij})\alpha_{ij}}{\sqrt{(s_{kl}-\alpha_{kl})(s_{kl}-\alpha_{kl})}}. \tag{31}$$

or in tensorial notation:

$$\begin{cases} H^{\mathrm{p}} \;=\; \sqrt{\frac{2}{3}}h - \eta_k\dfrac{(\boldsymbol{s}-\boldsymbol{\alpha})\colon\boldsymbol{\alpha}}{\sqrt{(\boldsymbol{s}-\boldsymbol{\alpha})\colon(\boldsymbol{s}-\boldsymbol{\alpha})}}, & (32) \\ H^{\mathrm{p}} \;=\; \sqrt{\frac{2}{3}}\left[h_i\exp\left(-\dfrac{h_i\bar{\varepsilon}^{\mathrm{p}}}{\sigma_u^{\infty}-\sigma_{\mathrm{y}}^0}\right)+h_k\right] \;-\; \eta_k\dfrac{(\boldsymbol{s}-\boldsymbol{\alpha})\colon\boldsymbol{\alpha}}{\sqrt{(\boldsymbol{s}-\boldsymbol{\alpha})\colon(\boldsymbol{s}-\boldsymbol{\alpha})}}. & (33) \end{cases}$$

It can be seen from these last two equations that the backstress tensor $\boldsymbol{\alpha}$ will play a major role in the behavior of the generalized plastic modulus H^{p}. The dynamic recovery parameter η_k characterizes how important the influence of the backstress tensor is in the value of H^{p}. Some limit cases that could be studied would be

- $\eta_k \;=\; 0$ (no dynamic recovery), which would actually lead to a linear kinematic hardening,
- η_k is such that $H^{\mathrm{p}} \;=\; 0$ at the end of the cycle (no hardening).

As it can be seen in Fig. 14 which represent the yield surface in Haigh Westergaard's space, the dynamic recovery term $-\eta_k\dot{\bar{\varepsilon}}^{\mathrm{p}}\alpha_{ij}$ is opposing the Bauschinger effect. So, it tends to reduce the value of the generalized plastic modulus H^{p}. It is linked to the fading memory effect which tends to reduce the backstress when it is non-zero.

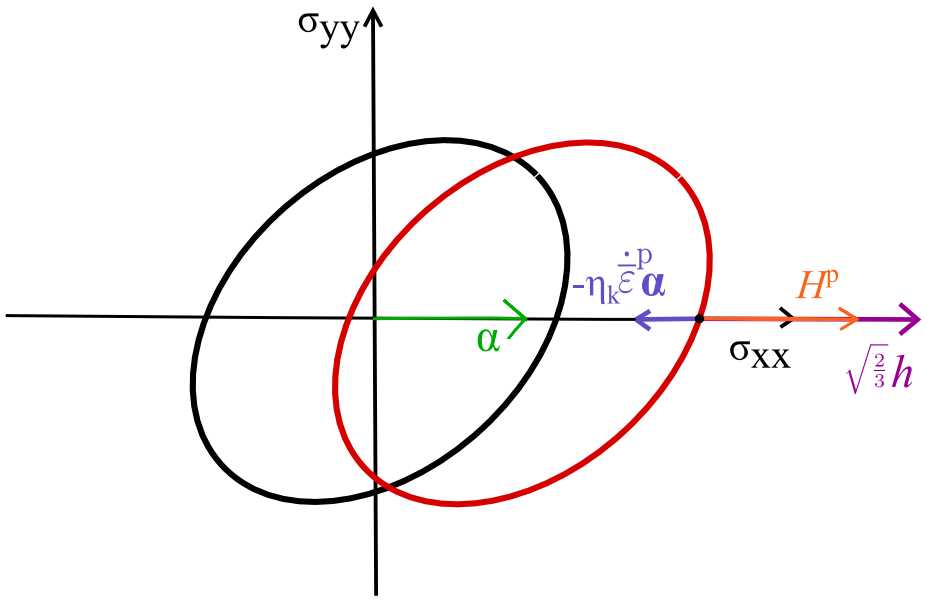

Fig. 14: Influence of the dynamic recovery term $-\eta_k \dot{\bar{\epsilon}}^{\mathrm{p}}$ on the generalized plastic modulus H^{p} represented schematically in the Haigh Westergaard's space. The black ellipse is the initial yield surface and the red ellipse is the yield surface that was shifted due to Bauschinger effect. The green arrow is the backstress, the blue arrow shows the effect of the dynamic recovery term, the orange one represents the generalized plastic modulus and the purple one is its positive term.

2.2 Analysis of the effect of the maximum load $t_{\max}$

For the analysis of the different types of nonlinear hardening, the value of η_k will have a fixed value, which was arbitrarily chosen so that it does not yield one of the limit cases. The chosen value is $\eta_k = \sqrt{\frac{2}{3}}\frac{h}{\sigma_{\mathrm{y}}^0}$. Furthermore, to compare and contrast them, the same type of loading and unloading cycles is applied but this time, the maximum surface load $t_{\max}$ will be varied and will be set to 250, 300, 350 and 400 [MPa].

Three types of hardening will be considered. The first and simplest one is the nonlinear kinematic hardening which is described by Armstrong Frederick's evolution law of the backstress tensor with no isotropic hardening. The second one combines the former with a linear isotropic hardening with a mixing parameter $\theta = 0.2$. The last one combined the first one with a nonlinear isotropic hardening described by Voce's saturated law and with the same mixing parameter.

From Fig. 15 to Fig. 19, the range of values shown along the vertical axis may be different for figures that are next to one another. Indeed, the main aim of these figures are not to show that the range of values for each type of hardening are different but to show the differences in the general behavior of each of them.

2.2.1 Analysis of the strain

The normal strain ε_{xx}'s behaviors are shown in Fig. 15. It can be noticed that the maximum load $t_{\max}$ has no influence whatsoever in the general behavior of the curves. The pure nonlinear kinematic hardening in Fig. 15a remains periodic with no change in amplitude. The combination with a linear

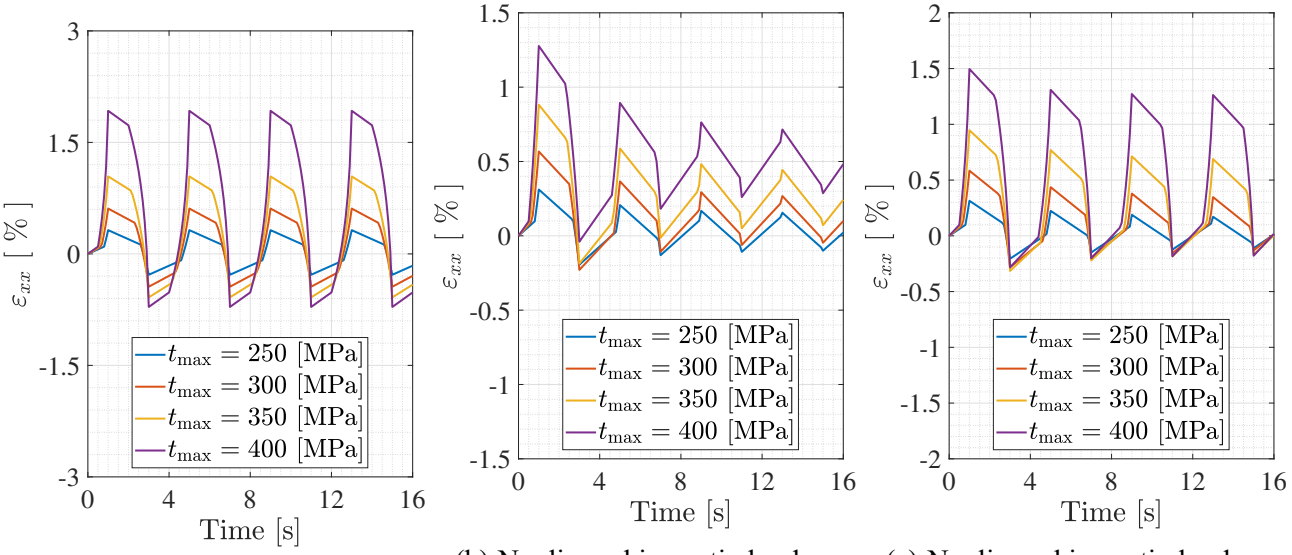

(a) Nonlinear kinematic hardening only.

(b) Nonlinear kinematic hardening combined with a linear kinematic hardening.

(c) Nonlinear kinematic hardening combined with a nonlinear kinematic hardening.

Fig. 15: Time evolution of the strain ε_{xx}, of the cube in plane stress state, at Node 7, in the direction parallel to the applied cyclic load. Four cycles of four seconds each are applied with a maximum load of respectively 250, 300, 350 and 400 [MPa]. The dynamic recovery parameter is set to $\eta_k = \sqrt{\frac{2}{3}}\frac{h}{\sigma_y^0}$. Three materials with different types of hardening are tested: (a) a nonlinear kinematic hardening with no added isotropic hardening, (b) a nonlinear kinematic hardening with a linear isotropic hardening and (c) a nonlinear kinematic hardening with a nonlinear isotropic hardening.

isotropic hardening in Fig. 15b has a fast decreasing amplitude and the variations from an extremum to another seem to be less an less steep with time. The combination with a nonlinear isotropic hardening in Fig. 15c has an amplitude that decreases less, seems to converge towards a non-zero value and seem to keep a self-similar profile.

In fact, the main influence of $t_{\max}$ is the amplitude, i.e. the bigger the maximum load, the bigger the amplitude, and the upward shift, i.e. the bigger the maximum load, the higher the value of the midline. This increases seem to follow some power law in the three cases. At this point, it can be inferred that the shift is due to the backstress.

The strain in the other directions ε_{yy} and ε_{zz} are not shown because they would lead to a similar analysis with no additional information.

The equivalent plastic strain $\bar{\varepsilon}^{\mathrm{p}}$'s behaviors are displayed in Fig. 16. Here also, the maximum load $t_{\max}$ plays a limited role in the general appearance of the curves, its influence is limited to only the numerical values, which are higher the higher the value of $t_{\max}$, and the time during which $\bar{\varepsilon}^{\mathrm{p}}$ increases: the higher the value of $t_{\max}$, the longer the increase lasts. The pure nonlinear kinematic hardening in Fig.16a has a repeating pattern and does not seem to converge. In contrast, the combination with a linear isotropic hardening in Fig. 16b converges fast. The combination with a nonlinear isotropic hardening in Fig. 16c also seems to have a decreasing increment after each cycle but does not seem to converge.

2.2.2 Analysis of the backstress

The normal backstress α_{xx} illustrated by Fig. 17 is not influenced, except for the amplitude, by the value of $t_{\max}$ at first sight. However, looking closely, the backstress also increases and decreases

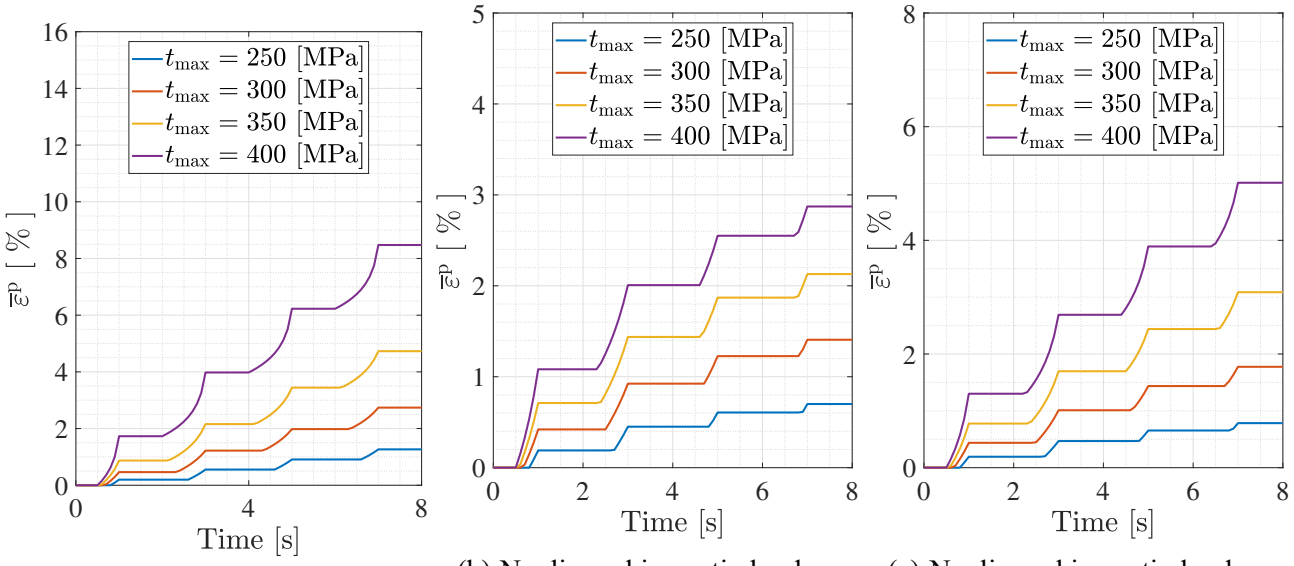

(a) Nonlinear kinematic hardening only.

(b) Nonlinear kinematic hardening combined with a linear kinematic hardening.

(c) Nonlinear kinematic hardening combined with a nonlinear kinematic hardening.

Fig. 16: Time evolution of the equivalent plastic strain $\bar{\varepsilon}^p$, of the cube in plane stress state, at Node 7. Two cycles of four seconds each are applied with a maximum load of respectively 250, 300, 350 and 400 [MPa]. The dynamic recovery parameter is set to $\eta_k = \sqrt{\frac{2}{3}}\frac{h}{\sigma_y^0}$. Three materials with different types of hardening are tested: (a) a nonlinear kinematic hardening with no added isotropic hardening, (b) a nonlinear kinematic hardening with a linear isotropic hardening and (c) a nonlinear kinematic hardening with a nonlinear isotropic hardening.

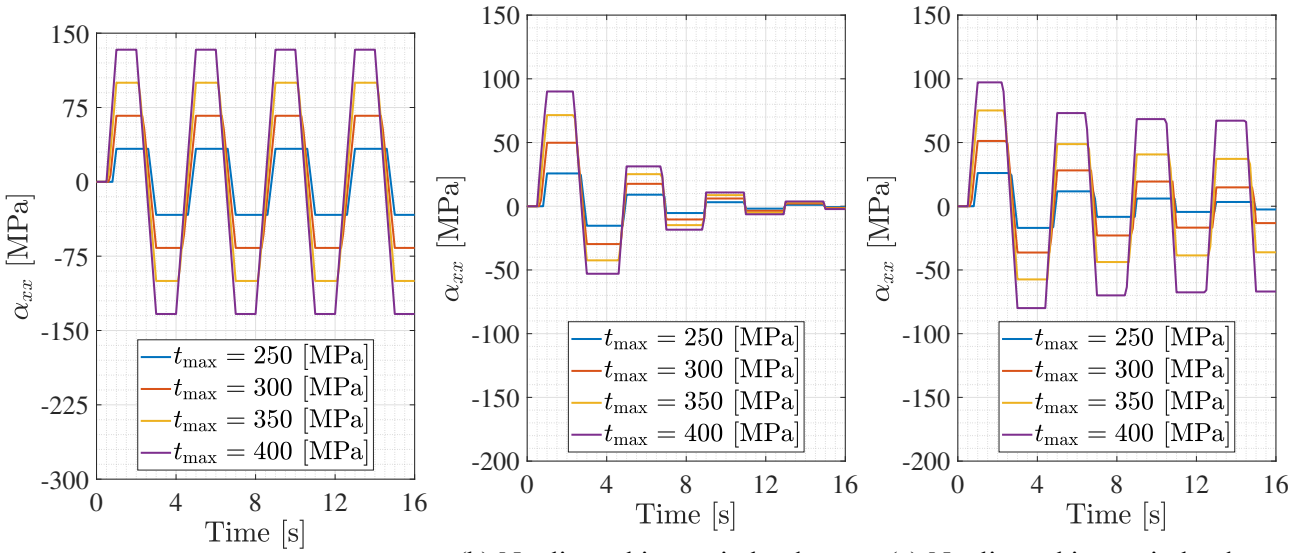

(a) Nonlinear kinematic hardening only.

(b) Nonlinear kinematic hardening combined with a linear kinematic hardening.

(c) Nonlinear kinematic hardening combined with a nonlinear kinematic hardening.

Fig. 17: Time evolution of the backstress α_{xx} of the cube in plane stress state, at Node 7, in the direction parallel to the applied cyclic load. Four cycles of four seconds each are applied with a maximum load of respectively 250, 300, 350 and 400 [MPa]. The dynamic recovery parameter is set to $\eta_k = \sqrt{\frac{2}{3}}\frac{h}{\sigma_y^0}$. Three materials with different types of hardening are tested: (a) a nonlinear kinematic hardening with no added isotropic hardening, (b) a nonlinear kinematic hardening with a linear isotropic hardening and (c) a nonlinear kinematic hardening with a nonlinear isotropic hardening.

earlier when the maximum load is higher. Be that as it may, the backstress for the pure nonlinear kinematic hardening in Fig. 17a remains periodic with time and similarly to the normal stress ε_{xx}, the combination with the linear isotropic hardening in Fig. 17b converges fast and the one with the nonlinear isotropic hardening in Fig. 17c seems to converge more slowly. All three types of hardening shows that the backstress oscillates around zero and eventually converges towards it in the second case but not necessarily in the third. That shows that in the cyclic loading, the Bauschinger effect will be eventually bested by the dynamic recovery of the fading memory effect.

Here also, the backstress in the perpendicular directions α_{yy} and α_{zz} are not shown because they would be analyzed in the similar way and would not bring any additional information.

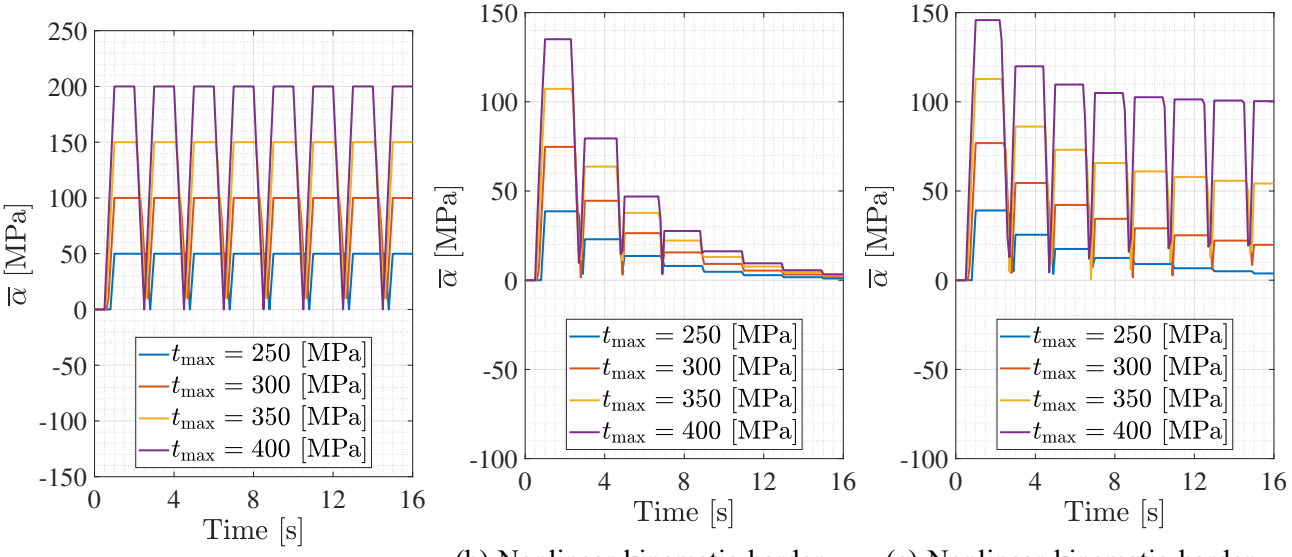

(a) Nonlinear kinematic hardening only.

(b) Nonlinear kinematic hardening combined with a linear kinematic hardening.

(c) Nonlinear kinematic hardening combined with a nonlinear kinematic hardening.

Fig. 18: Time evolution of the equivalent backstress $\overline{\alpha}$ of the cube in plane stress state, at Node 7. Four cycles of four seconds each are applied with a maximum load of respectively 250, 300, 350 and 400 [MPa]. The dynamic recovery parameter is set to $\eta_k = \sqrt{\frac{2}{3}}\frac{h}{\sigma_y^0}$. Three materials with different types of hardening are tested: (a) a nonlinear kinematic hardening with no added isotropic hardening, (b) a nonlinear kinematic hardening with a linear isotropic hardening and (c) a nonlinear kinematic hardening with a nonlinear isotropic hardening.

The equivalent backstress $\overline{\alpha}$'s evolution is shown in Fig. 18. Again here, $t_{\max}$ seems to play a limited role, mainly in the amplitude and the starting time of each increase and decrease of the equivalent backstress. Fig. 18a shows that the amplitude remains stable with time in the case of a pure nonlinear kinematic hardening contrary to the two other types of hardening. The mixed hardening with a linear isotropic hardening from Fig. 18b has an amplitude decreasing towards zero while the one with a nonlinear isotropic hardening in Fig. 18c has also a converging amplitude but not necessarily towards zero. That asymptotic value actually depends on $t_{\max}$.

So, Fig. 18c shows that in the third type of hardening, the equivalent backstress $\overline{\alpha}$ does not seem to always converge towards 0 when the number of cycles is increased towards infinity. In fact, it can be inferred that if the absolute value of the extrema of the loading/unloading cycles are below the asymptotic value of the yield stress σ_y^∞ from the nonlinear isotropic hardening law, then the backstress converge towards 0 like for the mixed hardening with the linear isotropic law in Fig.18b. That is because there is a moment when the material stops entering the plastic domain because the yield stress has become too high, so the backstress stops increasing and the dynamic recovery gets the backstress back to 0. However, if the load goes over that limit, then at each cycle from the start to infinity, the

material enters the plastic domain and the backstress always varies with fixed extrema like for the pure kinematic hardening in Fig 18a.

2.2.3 Analysis of the stress

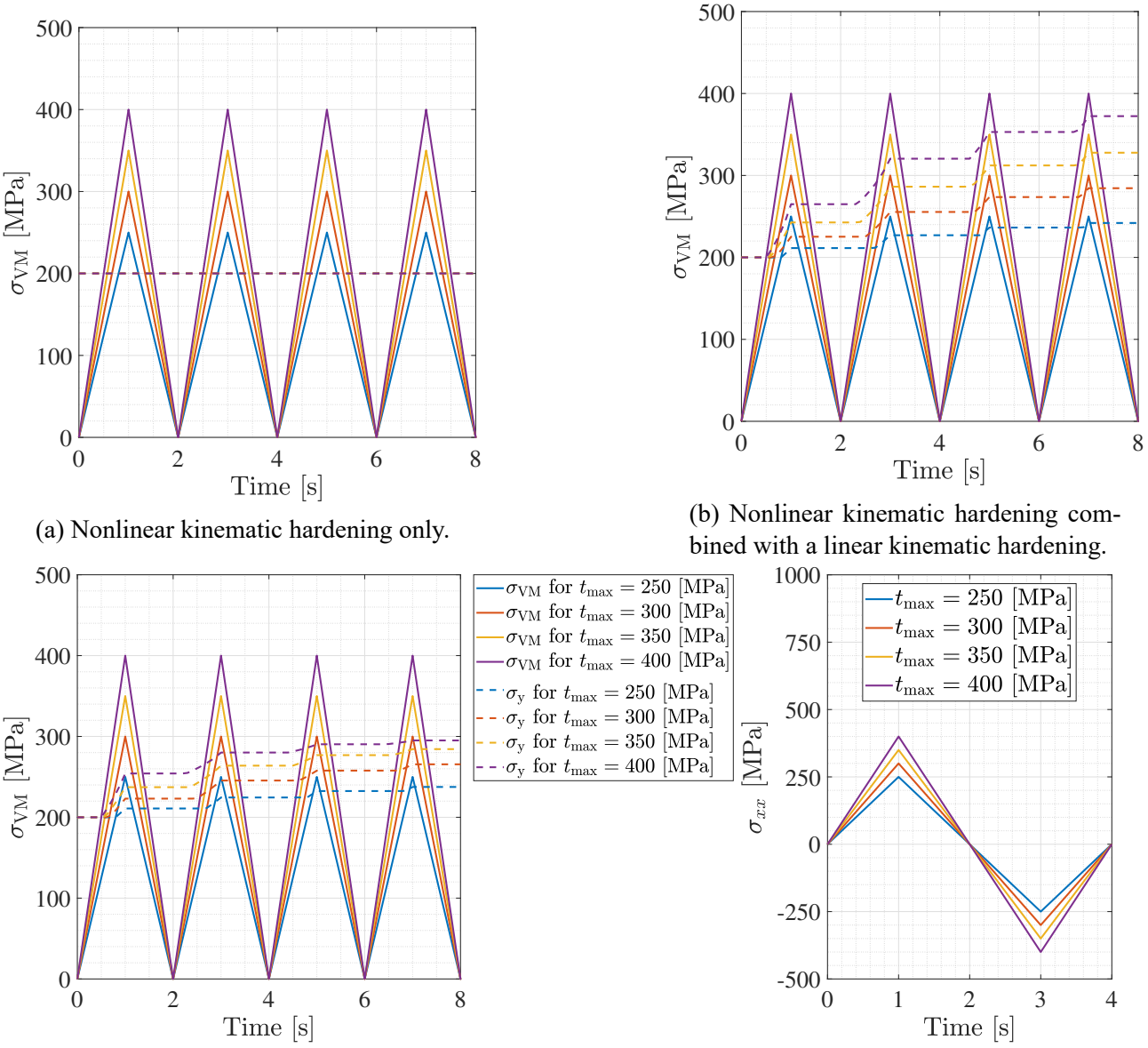

(a) Nonlinear kinematic hardening only.

(b) Nonlinear kinematic hardening combined with a linear kinematic hardening.

(c) Nonlinear isotropic hardening

(d) Axial stress

Fig. 19: Time evolution of three types of stress of the cube in plane stress state, at Node 7. Two cycles of four seconds each are applied in the first three figures and only one in the last but all were made with a maximum load of respectively 250, 300, 350 and 400 [MPa]. The dynamic recovery parameter is set to $\eta_k = \sqrt{\frac{2}{3}}\frac{h}{\sigma_y^0}$. The first three shows figures show the evolution of the Von Mises $\overline{\sigma}^{\text{VM}}$ stress in full lines and the yield stress σ_y in dashed lines. In the first figure, all dashed lines have collapsed into a single one. Three materials with different types of hardening are tested: (a) a nonlinear kinematic hardening with no added isotropic hardening, (b) a nonlinear kinematic hardening with a linear isotropic hardening and (c) a nonlinear kinematic hardening with a nonlinear isotropic hardening. The last figure shows (d) the axial stress, for all three types of hardening, in the direction parallel to the loading.

To conclude the study of the maximum load $t_{\max}$, the stress is analyzed in Fig. 19. For the Von Mises stresses $\overline{\sigma}^{\text{VM}}$ and the normal stress σ_{xx} , the only impact of $t_{\max}$ is an increase in amplitude for higher values of the maximum load. For the yield stress σ_{y}, on top of that, the time during which it increases is also longer. In pure nonlinear kinematic hardening displayed in Fig. 19a, the amplitude of the Von Mises stress is constant and the value of the yield stress does not not change, as in this type of hardening, there is no law describing its variation. In Fig. 19b, for the mixed hardening with a linear isotropic part, the same type of Von Mises stress is observed but the yield stress gradually increases until it reaches the value of the maximum load $t_{\max}$. A similar observation can be made for the combination with nonlinear isotropic hardening in Fig. 19c but the asymptotic value is not $t_{\max}$ but instead $\sigma_{\text{y}}^{\infty}$ which is a parameter of the nonlinear kinematic hardening. The normal stress represented in Fig. 19d is the same for all and, like the Von Mises stress, does not vary from a cycle to another. Hence, it was plotted once for all. As for the stress in the other directions σ_{yy} and σ_{zz}, they were observed to be negligible and were then not considered in this analysis.

Looking back at the evolution of the yield stress in Fig. 19b for the nonlinear kinematic hardening mixed with a linear isotropic hardening, when the material entered the plastic domain, the yield stress appeared to evolve linearly. Was it actually the case ? To answer this question, the evolution law for the yield stress for an isotropic hardening is used and given as follows:

$$\dot{\sigma}_{\text{y}} \;=\; h_i \dot{\bar{\varepsilon}}^{\text{p}} \;=\; \sqrt{\frac{2}{3}} h_i \lambda. \tag{34}$$

Knowing that the parameter h_i is constant, for the yield stress to evolve linearly, the plastic multiplier λ has to be constant. Let us develop the consistency equation in the case of non-linear kinematic hardening and linear isotropic hardening:

$$\dot{f} = \frac{\partial f}{\partial \sigma_{ij}} \dot{\sigma}_{ij} - \frac{\partial f}{\partial \sigma_{ij}} \dot{\alpha}_{ij} - \dot{\sigma}_y = 0 \tag{35}$$

$$\frac{\partial f}{\partial \sigma_{ij}} \dot{\sigma}_{ij} = \sqrt{\frac{3}{2}} N_{ij} \left(\frac{2}{3} h_k \lambda N_{ij} - \eta_k \sqrt{\frac{2}{3}} \lambda \alpha_{ij} \right) + h_i \sqrt{\frac{2}{3}} \lambda. \tag{36}$$

This gives us the expression of λ:

$$\lambda \;=\; \frac{1}{H^p} \frac{\partial f}{\partial \sigma_{ij}} \dot{\sigma}_{ij} \;=\; \frac{\partial f}{\partial \sigma_{ij}} \dot{\sigma}_{ij} \Big/ \left(\sqrt{\frac{2}{3}} h - \eta_k N_{ij} \alpha_{ij} \right). \tag{37}$$

The numerator is constant. To determine whether the denominator is constant or not, let us write its derivative knowing that N_{ij} is constant:

$$N_{ij} \dot{\alpha}_{ij} = N_{ij} \left(\frac{2}{3} h_k D_{ij}^{\text{p}} - \eta_k \dot{\bar{\varepsilon}}^{\text{p}} \alpha_{ij} \right) \tag{38}$$

$$= \frac{2}{3} h_k \lambda - \eta_k \sqrt{\frac{2}{3}} \lambda N_{ij} \alpha_{ij}. \tag{39}$$

This expression is certainly non-zero in general. Therefore, $N_{ij}\alpha_{ij}$ and consequently λ are not constant. We conclude that the yield stress does not evolve linearly.

2.2.4 Conclusion of the impact of $t_{\max}$

In short, with the exception of the amplitude, the maximum load $t_{\max}$ does not have an earth-shattering impact in the general behavior of the material with the three types of hardening. The only effect that is worth mentioning is the asymptotic value of the backstress, in the case of the nonlinear mixed hardening, i.e. combination of both nonlinear kinematic and nonlinear isotropic hardening.

2.3 Plastic dissipation

In Part 1, the expression of the plastic dissipation $\mathbb{D}$ was established. For the models considered in this part, the dissipation evolved linearly. In this subsection, the same steps will be followed and eventually, a similar expression will be obtained for the nonlinear kinematic hardening. Starting from Eq. 16 and inserting in it the expression found for λ from Eq. 37, the following expression is obtained:

$$\begin{aligned}\mathbb{D} &= \frac{1}{\sqrt{\frac{2}{3}}h - \eta_k N_{mn}\alpha_{mn}} \frac{\partial f}{\partial \sigma ij} \dot{\sigma_{ij}} \sigma_{kl} N_{kl} \\ &= \sqrt{\frac{3}{2}} \frac{\dot{\sigma_{ij}} N_{ij} \sigma_{kl} N_{kl}}{\sqrt{\frac{2}{3}}h - \eta_k N_{mn}\alpha_{mn}} \\ &= \frac{3}{2} \frac{\dot{\sigma_{ij}} N_{ij} \sigma_{kl} N_{kl}}{h - \sqrt{\frac{3}{2}}\eta_k N_{mn}\alpha_{mn}}. \end{aligned} \tag{40}$$

During the loading, $\dot{\sigma_{ij}}$ and all the N_{ij} remains constant, whereas σ_{kl} evolves linearly with time. However, if the isotropic hardening is nonlinear, then h is not constant, but because α_{mn} from the nonlinear kinematic hardening term is not constant, the dissipation $\mathbb{D}$ is in any case not linear with time, contrary to the linear kinematic hardening.

2.4 Evolutions in tensile and compression cycles

In order to get some insight on the behavior of the backstress. Some simple analytical laws will be made with respect to the plastic strain. Starting from Eq. 18, the backstress evolution law can be rewritten as follows:

$$\dot{\alpha}_{ij} = \frac{2}{3} h_k \dot{\varepsilon}^{\mathrm{p}}_{ij} - \eta_k \dot{\overline{\varepsilon}}^{\mathrm{p}} \alpha_{ij}. \tag{41}$$

The components of the backstress tensor α_{ij} were chosen such that $\overline{\alpha} = \sqrt{\frac{3}{2}\alpha_{ij}\alpha_{ij}} = |\alpha|$, i.e.

$$\alpha_{ij}\alpha_{ij} = \frac{2}{3}\alpha^2. \tag{42}$$

Then, applying a double inner product on Eq. 41 with α_{ij} yields successively

$$\dot{\alpha}_{ij}\alpha_{ij} = \frac{2}{3} h_k \dot{\varepsilon}^{\mathrm{p}}_{ij}\alpha_{ij} - \eta_k \dot{\overline{\varepsilon}}^{\mathrm{p}} \alpha_{ij}\alpha_{ij}, \tag{43}$$

$$\frac{1}{2}(\dot{\alpha_{ij}\alpha_{ij}}) = \frac{2}{3} h_k \dot{\varepsilon}^{\mathrm{p}}_{ij}\alpha_{ij} - \eta_k \dot{\overline{\varepsilon}}^{\mathrm{p}} (\alpha_{ij}\alpha_{ij}), \tag{44}$$

$$\frac{1}{3}\dot{\alpha^2} = \frac{2}{3} h_k \dot{\varepsilon}^{\mathrm{p}}_{ij}\alpha_{ij} - \frac{2}{3}\eta_k \dot{\overline{\varepsilon}}^{\mathrm{p}} \alpha^2, \tag{45}$$

$$2\alpha\dot{\alpha} = 2h_k \dot{\varepsilon}^{\mathrm{p}}_{ij}\alpha_{ij} - 2\eta_k \dot{\overline{\varepsilon}}^{\mathrm{p}} \alpha^2. \tag{46}$$

$$\tag{47}$$

In a tensile and compression cycle, $\dot{\varepsilon}^{\mathrm{p}}_{ij}\alpha_{ij} = \dot{\overline{\varepsilon}}^{\mathrm{p}}\alpha$, so the previous equation becomes

$$\dot{\alpha} = h_k \dot{\overline{\varepsilon}}^{\mathrm{p}} - \eta_k \dot{\overline{\varepsilon}}^{\mathrm{p}} \alpha = \dot{\overline{\varepsilon}}^{\mathrm{p}} (h_k - \eta_k \alpha). \tag{48}$$

The first order differential equation in α with respect to $\overline{\varepsilon}^{\mathrm{p}}$ is the obtained as follows:

$$\frac{\partial \alpha^{\mathrm{p}}}{\partial \overline{\varepsilon}} = h_k - \eta_k \alpha. \tag{49}$$

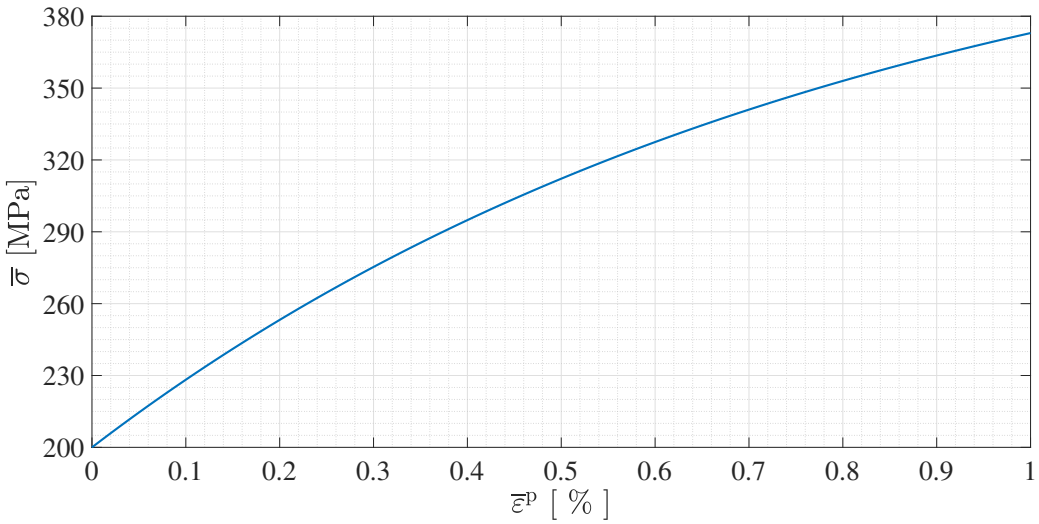

Fig. 20: Evolution of the equivalent stress $\overline{\sigma}$ with respect to the equivalent plastic strain $\overline{\varepsilon}^{\mathrm{p}}$ for tensile/compression cycles as it was defined in Eq. 54. The parameter used for η_k is the same as the one used in the whole section.

The general solution is given by

$$\alpha\left(\overline{\varepsilon}^{\mathrm{p}}\right) \;=\; \frac{h_k}{\eta_k} \;-\; C\, e^{-\eta_k \overline{\varepsilon}^{\mathrm{p}}}, \tag{50}$$

with C an arbitrary constant. If $\alpha = 0$ when $\overline{\varepsilon}^{\mathrm{p}} = 0$, then the final analytical expression is

$$\alpha\left(\overline{\varepsilon}^{\mathrm{p}}\right) \;=\; \frac{h_k}{\eta_k}\left(1 \;-\; e^{-\eta_k \overline{\varepsilon}^{\mathrm{p}}}\right). \tag{51}$$

This expression can then be used to determined the expression of the equivalent stress $\overline{\sigma}$ for the nonlinear kinematic hardening:

$$\begin{aligned}
\frac{d\overline{\sigma}}{d\overline{\varepsilon}^{\mathrm{p}}} \;&=\; \sqrt{\frac{3}{2}} H^{\mathrm{p}} \;=\; \frac{3}{2}\left[\sqrt{\frac{2}{3}} h_k \;-\; \eta_k N_{ij}\alpha_{ij}\right] && \text{(Using Eq. 31)} \\
&=\; \frac{3}{2}\left[\sqrt{\frac{2}{3}} h_k \;-\; \eta_k \sqrt{\frac{2}{3}}\alpha\right] && \text{(In tensile/compression cycles)} \\
&=\; h_k \;-\; h_k\left(1 \;-\; e^{-\eta_k \overline{\varepsilon}^{\mathrm{p}}}\right) \;=\; h_k e^{-\eta_k \overline{\varepsilon}^{\mathrm{p}}}.
\end{aligned} \tag{52}$$

Finally, the following expression is obtained:

$$\overline{\sigma} \;=\; D \;-\; \frac{h_k}{\eta_k} h_k e^{-\eta_k \overline{\varepsilon}^{\mathrm{p}}}, \tag{53}$$

where D is a constant. If $\overline{\sigma} = \sigma_{\mathrm{y}}^0$ when $\overline{\varepsilon}^{\mathrm{p}} = 0$, then it becomes

$$\overline{\sigma} \;=\; \sigma_{\mathrm{y}}^0 \;+\; \frac{h_k}{\eta_k}\left(1 \;-\; e^{-\eta_k \overline{\varepsilon}^{\mathrm{p}}}\right). \tag{54}$$

The resulting expression is plotted in Fig. 20 and it is a monotonic function. As such, the curve represent a closed cycle in the space $\overline{\sigma} - \overline{\varepsilon}^{\mathrm{p}}$.

2.5 Asymptotic values

Asymptotic values of the backstress tensor α_{ij} and the the yield stress σ_{y} can be determined from respectively Eq. 21 and both Eq. 2 and Eq. 22 with λ strictly positive.

The asymptotic value of the backstress α_{ij}^{u} is obtained when $\dot{\alpha_{ij}} = 0$. It yields that

$$0 \;=\; \frac{2}{3} h_k N_{ij} \;-\; \sqrt{\frac{2}{3}} \eta_k \alpha_{ij}. \tag{55}$$

Developing N_{ij} gives

$$\sqrt{\frac{2}{3}} h_k \frac{s_{ij} - \alpha_{ij}}{\sqrt{(s_{kl} - \alpha_{kl})(s_{kl} - \alpha_{kl})}} \;=\; \eta_k \alpha_{ij}. \tag{56}$$

Isolating α_{ij} to get an expression of α_{ij}^{u} gives

$$\alpha_{ij}^{\mathrm{u}} \;=\; \frac{s_{ij}}{1 + \frac{\eta_k}{h_k}\sqrt{\frac{3}{2}(s_{kl} - \alpha_{kl})(s_{kl} - \alpha_{kl})}} \;=\; \frac{s_{ij}}{1 + \frac{\eta_k}{h_k}\overline{\sigma}^{\mathrm{VM}}}, \tag{57}$$

with $\overline{\sigma}$ the effective yield stress. During the hardening, it is equal to σ_{y} and the solution becomes $\alpha_{ij}^{\mathrm{u}} = \frac{s_{ij}}{1 + \frac{\eta_k}{h_k}\sigma_{\mathrm{y}}}$. In Eq. 57, the higher the value of η_k, the smaller the value of α_{ij}^{u}. So, η_k earns well its name of dynamic recovery parameter.

In the case of a linear isotropic hardening, if $\dot{\sigma_{\mathrm{y}}} = 0$, then

$$0 \;=\; \sqrt{\frac{2}{3}} h_i, \tag{58}$$

so $h_i = 0$ and the asymptotic yield stress $\sigma_{\mathrm{y}}^{\mathrm{u}}$ has the value $\sigma_{\mathrm{y}}^{\mathrm{u}} = \sigma_{\mathrm{y}}^{0}$.

In the case of a nonlinear isotropic hardening, if $\dot{\sigma_{\mathrm{y}}} = 0$, then

$$0 \;=\; \sqrt{\frac{2}{3}} h_i \exp\left(-\frac{h_i}{\sigma_{\mathrm{y}}^{\infty} - \sigma_{\mathrm{y}}^{0}} \overline{\varepsilon}^{\mathrm{p}}\right), \tag{59}$$

which leads to two cases: either $h_i = 0$ and $\sigma_{\mathrm{y}}^{\mathrm{u}} = \sigma_{\mathrm{y}}^{0}$, or the exponential factor has a zero value and $\sigma_{\mathrm{y}}^{\mathrm{u}} = \sigma_{\mathrm{y}}^{\infty}$.

With these results, an upper bound of the equivalent stress $\sqrt{3J_2}$ can be found. From the definition of the Von Mises yield stress, the following can be written:

$$\left(\overline{\sigma}^{\mathrm{VM}}\right)^2 \;=\; \frac{3}{2}(s_{ij} - \alpha_{ij})(s_{ij} - \alpha_{ij}) \;=\; \frac{3}{2}(s_{ij}s_{ij} \;+\; \alpha_{ij}\alpha_{ij} \;-\; 2s_{ij}\alpha_{ij}). \tag{60}$$

$$\Leftrightarrow\; \frac{3}{2} s_{ij} s_{ij} \;=\; \left(\overline{\sigma}^{\mathrm{VM}}\right)^2 \;-\; \frac{3}{2}\alpha_{ij}\alpha_{ij} \;+\; 3 s_{ij}\alpha_{ij} \tag{61}$$

$$\leq\; \left(\overline{\sigma}^{\mathrm{VM}}\right)^2 \;+\; \frac{3}{2}\alpha_{ij}\alpha_{ij} \;+\; 3 s_{ij}\alpha_{ij} \qquad \text{(Using the triangular inequality)} \tag{62}$$

$$\leq\; \sigma_{\mathrm{y}}^2 \;+\; \overline{\alpha}^2 \;+\; 3 s_{ij}\alpha_{ij} \qquad \text{(During the hardening).} \tag{63}$$

Finally, an upper bound is given by

$$\sqrt{3J_2} \;\leq\; \sigma_{\mathrm{y}} \;+\; \overline{\alpha} \;+\; \sqrt{3 s_{ij}\alpha_{ij}}. \tag{64}$$

2.6 Conclusion

To conclude this part, the main results are gathered here. The nonlinear kinematic hardening has brought an additional dynamic recovery term to the law expressing the evolution of the backstress α. Its effect has been largely studied in the particular case of cyclic linear loading and unloading and it was confirmed that they changed the behavior of material if it is compared with the result from Part 1. When it is combined with an isotropic hardening, the extremum values of the backstress tend to decrease but in the case of the nonlinear one, the asymptotic value depends on the maximum magnitude of the load. Further, it was shown, that nonlinearities arise and complexifies the expression of certain values, such as the plastic dissipation. Finally, it was demonstrated that even if a nonlinear term was introduced, simple laws and asymptotic values could be found.

In the next section, viscosity effects will be introduced and will complexify even further the analysis.

3 Part 3: Study of elasto-viscoplastic behavior

In this part, we study the the elasto-viscoplastic behavior of the cube. We consider isotropic linear hardening and mixed linear hardening combined, combined with Perzyna's law for viscosity. Perzyna law states that

$$\lambda = \sqrt{\frac{3}{2}} \left\langle \frac{\overline{\sigma}^{\text{VM}} - \sigma_{\text{y}}}{\eta} \right\rangle = \sqrt{\frac{3}{2}} \left\langle \frac{f}{\eta} \right\rangle, \tag{65}$$

where $\langle \cdot \rangle$ are Mc Auley brackets, i.e.

$$\langle x \rangle = \begin{cases} x & \text{if } x \geq 0, \\ 0 & \text{if } x < 0. \end{cases} \tag{66}$$

Another formulation can be constructed when f is positive by defining an *extended* yield function $\overline{f}$:

$$\overline{f} = f - \eta \dot{\overline{\varepsilon}}^{\text{vp}}. \tag{67}$$

It may be worth noting that the Kuhn-Tucker conditions remain valid for all processes. This means we have

$$\lambda \overline{f} = 0, \quad \lambda \geq 0, \quad \overline{f} \leq 0, \tag{68}$$

for all processes. We still have the same categorization of the processes depending on whether the (extended) yield function is zero or not. If $\overline{f} < 0$, we are in the elastic domain and there is no viscoplastic flow. If $\overline{f} = 0$, we are in the viscoplastic domain. An important remark to make is that when in the elastic domain, $\lambda = 0$ and $\overline{f} = f$. This means that the first entrance into plasticity of the cube is not delayed by the viscosity.

Since f has the units of a pressure and $\overline{\varepsilon}^{\text{vp}}$ is dimensionless, the viscosity parameter η has for units MPa $\cdot$ s. Its dimensions are those of a mass per length per unit time ($\text{ML}^{-1}\text{T}^{-1}$).

3.1 A first example: constant imposed loading after a loading/unloading cycle

In order to study the viscoplasticity in the cube, we will examine a simple case worthy of being studied. After the cube has undergone a full loading/unloading cycle, the imposed load is kept at a constant non-zero value for a long time. The analysis of this example shall remain purely qualitative and based solely on simulations performed with metafor. Those simulations are performed with the maximal load in the cycle being t_{max} and $T_{\text{cycle}} = 4$ [s], in a state of plane stress. The influence of viscosity on the behavior of the cube remains qualitatively the same in plane strain as in plane stress. The main idea of this first example is to get some physical insight on the influence of viscosity on the behavior of the cube. An analytical study will be performed in the next sections.

As it shall be seen in next section, the quantity η/h, which has the units of a time, plays an important role in the time response to a static loading. Let us choose two values for this characteristic time: 0.2 [s] and 3 [s]. The first value is one fifth of the time taken by the loading to go from 0 to t_{max} (T_{cycle} is equal to 4 [s]). The second value is 3 times that time. The values so chosen should provide two significantly different results.

Fig. 21 represents $\overline{\sigma}^{\text{VM}}$, σ_{xx} and $\sigma_{\text{Yield}} = \sigma_y + \eta \dot{\overline{\varepsilon}}^{\text{vp}}$ for both isotropic and mixed linear hardening. This stress σ_{Yield} is the yield stress returned by metafor. As far as we know, there's no mean to access the "true" yield stress σ_y that would have carried a lot more information.[1] Since in the elastic region $\overline{f} < 0$ and therefore $\lambda = 0$, we have $\sigma_{\text{Yield}} = \sigma_y$. In the viscoelastic region, $\overline{f} = 0$ and we have $\sigma_{\text{Yield}} = \overline{\sigma}^{\text{VM}}$. Fig. 22 shows the equivalent viscoplastic strain $\overline{\varepsilon}^{\text{vp}}$ and the strain ε_{xx}. These two values depend on η. Fig. 23 represents the equivalent backstress in the case of mixed linear hardening.

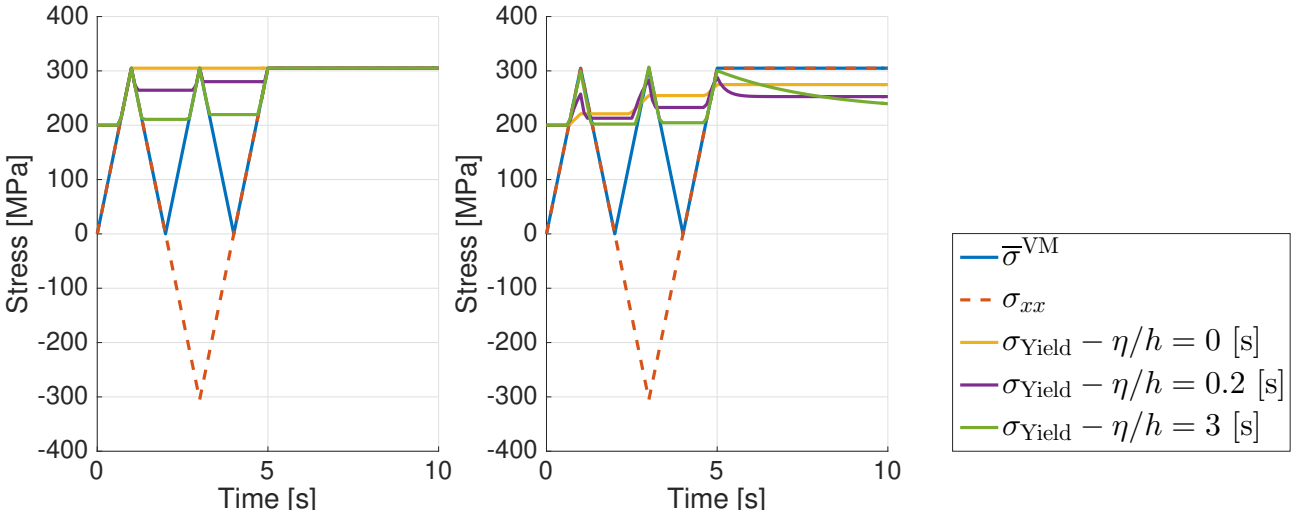

Fig. 21: Time evolution of $\overline{\sigma}^{\mathrm{VM}}$, σ_{xx} and of $\sigma_{\mathrm{Yield}} = \sigma_y + \eta\dot{\overline{\varepsilon}}^{\mathrm{vp}}$ for various value of the viscosity parameter η. The applied load describes a loading/unloading cycle and afterwards is maintained at the constant value $t_{\max}$. On the left figure, linear isotropic hardening is used. On the right figure, linear mixed hardening is used.

Let us start with the analysis of the case where linear isotropic hardening is used, as it is by far the most simple case. The stresses $\overline{\sigma}^{\mathrm{VM}}$ and σ_{xx} are independent of the viscosity parameter η. This is due to the fact that the load is imposed. However, as its definition suggests, σ_{Yield} depends on η. It can be observed on the graph that, after each peak of $\overline{\sigma}^{VM}$, the value of σ_{Yield} has increased by some amounts. Whereas, when no viscosity is considered, the yield stress attain its maximum value at the first peak of the von Mises stress. We can say that in some sense the viscosity delays the hardening of the material. If we take a look at the equivalent viscoplastic strain (Fig. 22), we see that a bigger viscosity parameter results in a smaller increase in $\overline{\varepsilon}^{\mathrm{vp}}$ after each peak of $\overline{\sigma}^{\mathrm{VM}}$. The viscosity has no influence on the final value of $\overline{\varepsilon}^{\mathrm{vp}}$. We also observe that during the static loading $\overline{\varepsilon}^{\mathrm{vp}}$ converges towards its final value by following a decreasing exponential. The higher the viscosity, the slower is this convergence. The fact that the equivalent viscoplastic strain converges towards a finite value indicates that its derivative $\dot{\overline{\varepsilon}}^{\mathrm{vp}}$ tends towards zero. After an infinite time, the viscosity term in the extended yield function vanishes and we have $\sigma_y = \overline{\sigma}^{\mathrm{VM}}$. In regard to all of these observations, we may conclude that the viscosity has a delaying and transient effect on the hardening of the linear isotropic hardening model.

Let us consider the influence of viscosity on the mixed linear hardening model. First of all, we see that a larger viscosity parameter results in a smaller increase in σ_{Yield} after each peak of the von Mises stress. We had already observed this behavior with the isotropic hardening. However the final value of σ_{Yield} depends on η. More viscosity induces a smaller final value of σ_{Yield}. By examining Fig. 22, we observe the same phenomenon for $\overline{\varepsilon}^{\mathrm{vp}}$. For a larger viscosity parameter, the equivalent viscoplastic strain increases slower and its final value is lower. As for the isotropic hardening, at infinity $\dot{\overline{\varepsilon}}^{\mathrm{vp}}$ tends towards zero and we retrieve $\sigma_y = \overline{\sigma}^{\mathrm{VM}}$. Since $\overline{\varepsilon}^{\mathrm{vp}}$ is smaller for a larger η, σ_y is smaller. Therefore we must have a smaller von Mises stress $\overline{\sigma}^{\mathrm{VM}} = \sqrt{\frac{3}{2}(s_{ij} - \alpha_{ij}) \cdot (s_{ij} - \alpha_{ij})}$. The loading being independant of the viscosity, this can only be satisfied by a "larger" backstress tensor. This is indeed what we observe on Fig. 23.

[1] We later discovered that we could retrieve the value of $\dot{\overline{\varepsilon}}^{\mathrm{vp}}$ from metafor and therefore the value of σ_y. Unfortunately we were too short on time, to make changes.

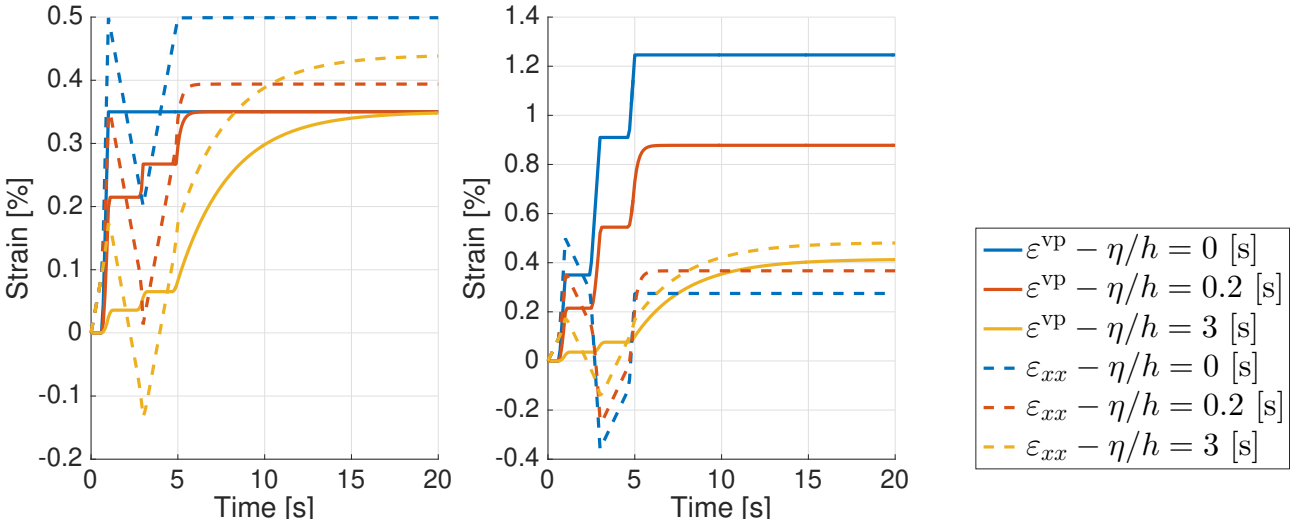

Fig. 22: Time evolution of $\overline{\varepsilon}^{\mathrm{vp}}$ and of ε_{xx} for various value of the viscosity parameter η. The applied load describes a loading/unloading cycle and afterwards is maintained at the constant value $t_{\max}$. On the left figure, linear isotropic hardening is used. On the right figure, linear mixed hardening is used. Attention must be paid to the fact that the ordinate value ranges for isotropic and mixed hardening are *not* the same.

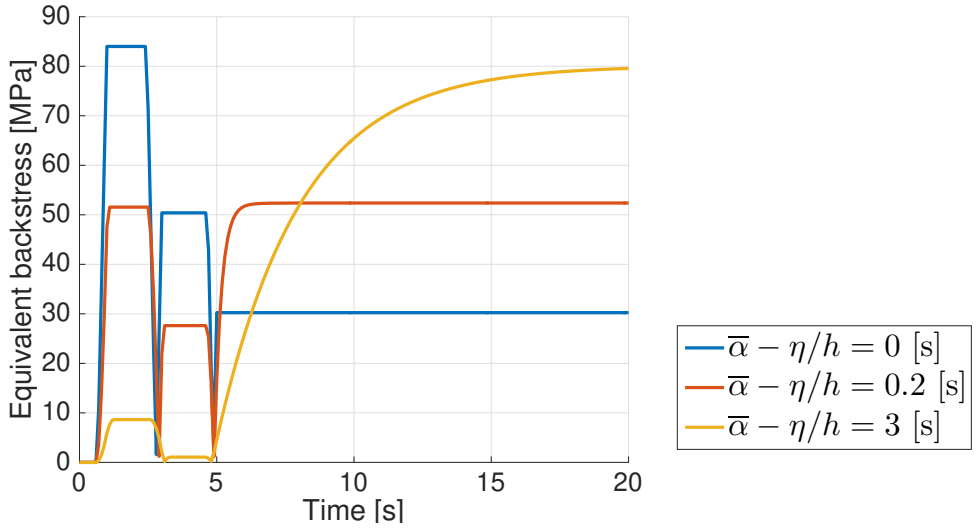

Fig. 23: Time evolution of the equivalent backstress $\overline{\alpha}$ for various value of the viscosity parameter η. The applied load describes a loading/unloading cycle and afterwards is maintained at the constant value $t_{\max}$. Linear mixed hardening is used.

3.2 A second example: ramp loading followed by constant loading

In this second example, the applied loading follows a ramp and after some time becomes constant. It stays constant for an *infinitely* long time. We will focus our attention on what happens *after* the ramp, during the constant loading.The equivalent Von Mises stress induced by the constant loading is σ^*_{VM}. Let us call t^* the time at which the constant load starts to be applied. In all the following, a quantity with the superscript $\cdot^*$ denotes the value of the quantity evaluated at time t^*. We assume that at time t^* the system is in such a state that it's in the viscoplastic domain and therefore that $f^* = \overline{\sigma}^{\text{VM}*} - \left(\sigma_y^0 + h_i \overline{\varepsilon}^{\text{vp}*}\right) > 0$. Let us develop the extended consistency equation in the general case of mixed hardening:

$$\begin{aligned}
& \dot{\overline{f}} = \frac{\partial \overline{f}}{\partial \sigma_{ij}} \dot{\sigma}_{ij} + \frac{\partial \overline{f}}{\partial \alpha_{ij}} \dot{\alpha}_{ij} - \dot{\sigma}_y - \eta \dot{\overline{\varepsilon}}^{\text{vp}} = 0 \\
\Leftrightarrow \quad & \frac{\partial \overline{f}}{\partial \sigma_{ij}} \dot{\sigma}_{ij} = \frac{\partial \overline{f}}{\partial \sigma_{ij}} \dot{\alpha}_{ij} + \dot{\sigma}_y + \eta \dot{\overline{\varepsilon}}^{\text{vp}} \\
\Leftrightarrow \quad & \frac{\partial \overline{f}}{\partial \sigma_{ij}} \dot{\sigma}_{ij} = \frac{2}{3} \lambda h_k N_{ij} \frac{\partial \overline{f}}{\partial \sigma_{ij}} + \lambda \sqrt{\frac{2}{3}} h_i + \eta \dot{\lambda} \sqrt{\frac{2}{3}}.
\end{aligned} \tag{69}$$

Since the imposed loading is constant, so is the stress in the cube and $\dot{\sigma}_{ij} = 0$. We recall that $\partial \overline{f} / \partial \sigma_{ij} = \sqrt{\frac{3}{2}} N_{ij}$. Further developments lead to:

$$\begin{aligned}
& \eta \dot{\lambda} \sqrt{\frac{2}{3}} = -\lambda \left[\sqrt{\frac{2}{3}} \left(h_i + h_k \right) \right] \\
\Leftrightarrow \quad & \dot{\lambda} = -\lambda \frac{h}{\eta}.
\end{aligned} \tag{70}$$

If we consider an elastic perfectly plastic material, h is equal to zero and we have $\dot{\lambda} = 0$. The solution of this differential equation is straightforward and using $\lambda(t^*) = \lambda^*$ we get $\lambda(t) = \lambda^*$ for all $t > t^*$. The equivalent viscoplastic strain is equal to $\overline{\varepsilon}^{\text{vp}}(t) = \overline{\varepsilon}^{\text{vp}*} + \lambda^* t$ for all $t > t^*$. We see that the cube will deform continuously, at a constant rate, until failure or at least until the model becomes totally inaccurate. An analogy to this model is the dash pot. When a constant force is applied on the dash pot, it deforms at a constant rate until infinity... or until it's no more a dash pot.

Let us now consider linear hardening. Whether it is isotropic or mixed has no influence on λ. Solving Eq. (70) with the same initial condition as before yields

$$\lambda(t) = \lambda^* \exp\left(-\frac{h}{\eta} (t - t^*) \right). \tag{71}$$

The equivalent viscoplastic strain is given by:

$$\overline{\varepsilon}^{\text{vp}} = \sqrt{\frac{2}{3}} \int_{t^*}^{t} \lambda(\tau) d\tau + \overline{\varepsilon}^{\text{vp}*} = \overline{\varepsilon}^{\text{vp}*} + \sqrt{\frac{2}{3}} \frac{\lambda^* \eta}{h} \left[1 - \exp\left(-\frac{h}{\eta} (t - t^*) \right) \right]. \tag{72}$$

In the previous section we observed that $\overline{\varepsilon}^{\text{vp}}$ follows a decreasing exponential during the static loading. This is exactly what we just obtained analytically. Moreover, we can deduce from the analytical expression that the evolution of $\overline{\varepsilon}^{\text{vp}}$ is exactly the same whether isotropic linear hardening or mixed linear hardening is considered. This result would have been much less obvious if we had considered the simulations only.

We see that we can form a characteristic time η/h. This time is characteristic of the duration of the viscosity effects. After $3 \cdot \eta/h$ seconds, the equivalent viscoplastic strain has attained 95% of its

final value. And after $4 \cdot \eta/h$ seconds it has attained 98%. Taking a smaller value for η results in a faster convergence as it was observed in the previous section.

In the case of isotropic linear hardening, the yield stress is given by:

$$\sigma_y = \sigma_y^0 + h\overline{\varepsilon}^{\text{vp}} = \sigma_y^0 + h\overline{\varepsilon}^{\text{vp}*} + \sqrt{\frac{2}{3}}\lambda^*\eta\left[1 - \exp\left(-\frac{h}{\eta}(t-t^*)\right)\right]. \tag{73}$$

Whereas in the case of mixed linear hardening, it is given by:

$$\sigma_y = \sigma_y^0 + h_i\overline{\varepsilon}^{\text{vp}} = \sigma_y^0 + h_i\overline{\varepsilon}^{\text{vp}*} + \frac{h}{h_i}\sqrt{\frac{2}{3}}\lambda^*\eta\left[1 - \exp\left(-\frac{h}{\eta}(t-t^*)\right)\right]. \tag{74}$$

Let us now seek the expression of the equivalent back-stress. The evolution of the back-stress tensor is governed by:

$$\dot{\alpha}_{ij} = \frac{2}{3}h_k D_{ij}^{\text{vp}} = \frac{2}{3}h_k N_{ij}. \tag{75}$$

Since the loading is constant, N_{ij} is constant and we have

$$\alpha_{ij} = \frac{2}{3}h_k N_{ij}\int_{t^*}^{t}\lambda(\tau)d\tau = \frac{2}{3}h_k \Lambda N_{ij}, \tag{76}$$

where we defined Λ as $\Lambda(t) = \int_{t^*}^{t}\lambda(\tau)d\tau$. We can write:

$$\begin{aligned} \overline{\alpha} &= \sqrt{\frac{3}{2}\alpha_{ij}\alpha_{ij}} = \sqrt{\frac{2}{3}}h_k\Lambda \\ \Rightarrow \quad \alpha_{ij} &= \sqrt{\frac{2}{3}}\overline{\alpha}N_{ij}. \end{aligned} \tag{77}$$

We can derivate the equivalent back-stress with respect to time:

$$\dot{\overline{\alpha}} = \sqrt{\frac{3}{2}}\frac{\alpha_{ij}\dot{\alpha}_{ij}}{\overline{\alpha}} \tag{78}$$

and using the expression of the back-stress tensor we just found we get:

$$\dot{\overline{\alpha}} = \frac{2}{3}h_k\lambda = \sqrt{\frac{2}{3}}h_k\dot{\overline{\varepsilon}}^{\text{vp}}. \tag{79}$$

Integrating $\dot{\overline{\alpha}}$ yields:

$$\begin{aligned} \overline{\alpha} &= \overline{\alpha}^* + \int_{t^*}^{t}\dot{\overline{\alpha}}(\tau)d\tau \\ &= \overline{\alpha}^* + \frac{2}{3}h_k\lambda^*\int_{t^*}^{t}\exp\left(-\frac{h(\tau-t^*)}{\eta}\right)d\tau \\ &= \overline{\alpha}^* + \frac{2}{3}h_k\frac{\lambda^*\eta}{h}\left[1 - \exp\left(-\frac{h(t-t^*)}{\eta}\right)\right]. \end{aligned} \tag{80}$$

3.3 A third example: loading/unloading at constant speed

In this subsection, we study analytically the elasto-viscoplastic behavior of the cube when submitted at a loading at constant speed and then followed by an unloading at constant speed. Mathematically, the loading function is defined as:

$$p(t) = \begin{cases} t_{\max}\frac{t}{t_1}, & \text{if } 0 < t < t_1, \\ t_{\max}\frac{t_1 - t}{t_3 - t_1}, & \text{if } 0 < t < t_3. \end{cases} \tag{81}$$

Let us note t_0 and t_2 the time where we enter/exit the viscoplastic region. We define the loading speed as the ratio $t_{\max}/t_1$ or, in more general manner, as the time derivative of the loading function. The units of this so-defined loading speed are MPa/s.

In the previous subsection, we had already developed the extended consistency criterion:

$$\frac{\partial \overline{f}}{\partial \sigma_{ij}} \dot{\sigma}_{ij} = \frac{2}{3} \lambda h_k N_{ij} \frac{\partial \overline{f}}{\partial \sigma_{ij}} + \lambda \sqrt{\frac{2}{3}} h_i + \eta \dot{\lambda} \sqrt{\frac{2}{3}}. \tag{82}$$

We may restate this as

$$\dot{\lambda} = -\lambda \frac{h}{\eta} + \frac{3}{2} \dot{\sigma}_{ij} N_{ij} \frac{1}{\eta}, \tag{83}$$

where we used the fact that $\partial \overline{f}/\partial \sigma_{ij} = \sqrt{3/2} N_{ij}$. This equation holds when in the viscoplastic region, i.e. when $t_0 < t < t_2$. Solving it for $t_0 < t < t_1$ yields

$$\lambda = \frac{3}{2} \frac{\dot{\sigma}_{ij} N_{ij}}{h} \left[1 - \exp\left(-\frac{h(t - t_0)}{\eta} \right) \right]. \tag{84}$$

We observe that there is a linear relationship between λ and $\dot{\sigma}_{ij}$ and thus between the equivalent viscoplastic strain and the loading speed. If we have $\eta \gg h(t_1 - t_0)$, we may expand the exponential in Taylor series. We get:

$$\lambda = \frac{3}{2} \frac{\dot{\sigma}_{ij} N_{ij}}{\eta} (t - t_0). \tag{85}$$

This is a limit case. We will refer to this limit case as the *viscosity dominated regime*. By a direct integration, we see that the equivalent viscoplastic strain $\bar{\varepsilon}^{\text{vp}}$ increases quadratically with the time spent in the viscoplastic region.

When the unloading starts, we do not immediately exit the viscoplastic region to regain the elastic region. The value of λ has first to decrease back to zero. If we denote by λ_1 the value taken by λ at time t_1, we have

$$\lambda = \lambda_1 \exp\left(-\frac{h(t - t_1)}{\eta} \right) + \frac{3}{2} \frac{\dot{\sigma}_{ij} N_{ij}}{h} \left[1 - \exp\left(-\frac{h(t - t_1)}{\eta} \right) \right]. \tag{86}$$

In the viscosity dominated regime, this becomes:

$$\lambda = \lambda_1 \left(1 - \frac{h(t - t_1)}{\eta} \right) + \frac{3}{2} \frac{\dot{\sigma}_{ij} N_{ij}}{\eta} (t - t_1). \tag{87}$$

Let us search for the value of t_2. By definition, at $t = t_2$, we have $\lambda = 0$. Let us develop that equality:

$$\begin{aligned} & 0 = \lambda_1 \exp\left(-\frac{h(t_2 - t_1)}{\eta} \right) + \frac{3}{2} \frac{\dot{\sigma}_{ij} N_{ij}}{h} \left[1 - \exp\left(-\frac{h(t_2 - t_1)}{\eta} \right) \right] \\ \Leftrightarrow \quad & \exp\left(-\frac{h(t_2 - t_1)}{\eta} \right) = \frac{\frac{3}{2} \dot{\sigma}_{ij} N_{ij} / h}{\frac{3}{2} \dot{\sigma}_{ij} N_{ij} - \lambda_1} \\ \Leftrightarrow \quad & t_2 = t_1 + \frac{\eta}{h} \ln\left(1 - \frac{2}{3} \frac{\lambda_1 h}{\dot{\sigma}_{ij} N_{ij}} \right) \end{aligned} \tag{88}$$

Let us insert the expression of λ_1 in it (that we can get from Eq. (84)). Attention must be paid to the fact that, even though N_{ij} hasn't change between the loading and the unloading stages, $\dot{\sigma}_{ij}$ changes sign when going from the loading to the unloading stage. We shall therefore use the absolute value

of $\dot{\sigma}_{ij}N_{ij}$. During the loading stage, we have $\dot{\sigma}_{ij}N_{ij} > 0$. During the unloading, we have $\dot{\sigma}_{ij}N_{ij} < 0$. We have

$$\begin{aligned} t_2 &= t_1 + \frac{\eta}{h}\ln\left(1 + \frac{2}{3}\frac{\lambda_1 h}{|\dot{\sigma}_{ij}N_{ij}|}\right) \\ &= t_1 + \frac{\eta}{h}\ln\left[2 - \exp\left(-\frac{h(t_1 - t_0)}{\eta}\right)\right]. \end{aligned} \tag{89}$$

In the viscosity dominated regime, we can expand this expression in Taylor series. We obtain:

$$\begin{aligned} t_2 &= t_1 + \frac{\eta}{h}\ln\left(1 + \frac{h(t_1 - t_0)}{\eta}\right) \\ &= 2t_1 - t_0. \end{aligned} \tag{90}$$

This can be restated as $t_2 - t_1 = t_1 - t_0$. The time spent in the viscoplastic region during the unloading is equal to the time spent in the viscoplastic region during the loading. This can observed in Fig. 21. For the largest value of η/h, we see that the two time are almost equal.

When taking the limit $\lim_{\eta\to 0} t_2$, we get:

$$\lim_{\eta\to 0} t_2 = t_1 + \lim_{\eta\to 0}\frac{\eta}{h}\ln(2) = t_1. \tag{91}$$

We recover the elasto-plastic behavior where we exit the elastic region as soon as the unloading starts.

3.4 Study of the signed distance to the yield surface with respect to the yield surface center

A variable with great physical significance is the overstress $d = \overline{\sigma}^{\text{VM}} - \sigma_y$. This can be seen as the signed distance to the yield surface with respect to the yield surface center. In the viscoplastic region, we have $\overline{f} = \overline{\sigma} - \sigma_y - \eta\dot{\overline{\varepsilon}}^{\text{vp}} = 0$. It follows that $d = \sqrt{\frac{2}{3}}\eta\lambda$. Re-using the results obtained during the previous section, the overstress during a loading/unloading cycle is given by:

$$d = \begin{cases} \sqrt{\frac{3}{2}}\frac{\dot{\sigma}_{ij}N_{ij}\eta}{h}\left[1 - \exp\left(-\frac{h(t-t_0)}{\eta}\right)\right] & \text{during the loading,} \\ \sqrt{\frac{3}{2}}\frac{|\dot{\sigma}_{ij}N_{ij}|\eta}{h}\Bigg\{\left[1 - \exp\left(-\frac{h(t_1-t_0)}{\eta}\right)\right]\exp\left(-\frac{h(t-t_1)}{\eta}\right) - & \\ \qquad - \left[1 - \exp\left(-\frac{h(t-t_1)}{\eta}\right)\right]\Bigg\}, & \text{during the unloading,} \end{cases} \tag{92}$$

where the times t_0, t_1 are those defined in the previous section. This expression of d holds for both traction and compression. The second formula for d holds until $t = t_2$, where t_2 is as found in the previous section.

The maximal overstress d_{max} is attained when the unloading starts, i.e. when the loading attains its maximum t_{max}. We have:

$$d_{\text{max}} = \sqrt{\frac{3}{2}}\frac{\dot{\sigma}_{ij}N_{ij}\eta}{h}\left[1 - \exp\left(-\frac{h(t_1 - t_0)}{\eta}\right)\right] \tag{93}$$

The maximal overstress depends in two ways on the loading speed. The first way is explicit through the term $\dot{\sigma}_{ij}$. This dependance is linear. The second way is implicitly through the term $t_1 - t_0$ in the exponential. The time interval $t_1 - t_0$ is inversely proportional to the loading speed. If the loading speed is increased, the term $1 - \exp(-h(t_1 - t_0)/\eta)$ decreases. In general, we connat conclude that

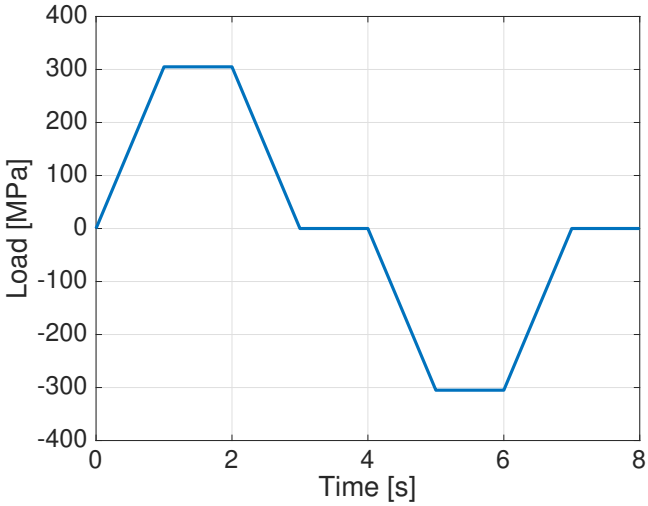

Fig. 24: Loading function, smoothened version of the saw tooth

increasing the loading speed will result in an increase in $d_{\max}$. In the viscosity dominated regime, we can expand the exponential in Taylor series. This leads to:

$$d_{\max} = \sqrt{\frac{3}{2}}\dot{\sigma}_{ij}N_{ij}(t_1 - t_0). \tag{94}$$

Since $t_1 - t_0$ is inversely proportional to the loading speed, $d_{\max}$ is constant with respect to the loading speed. If we recall Fig. 21, we observed that, after a loading/unloading (in traction or in compression), the yield stress does not increase significantly if the viscosity parameter is large enough. We may extrapolate this observation by stating that the yield stress is almost constant during the time spent in the viscoplastic region and the maximal overstress is given by $d_{\max} = \overline{\sigma}^{\text{VM}}_{\max} - \sigma_y^*$, where $\overline{\sigma}^{\text{VM}}_{\max}$ is the von Mises stress when loading is equal to $t_{\max}$ and where σ_y^* is the yield stress before entering the viscoplastic region. This result can be recovered in another way. We still assume that σ_y is almost constant. The maximal overstress can be obtained by integrating its derivative:

$$\begin{aligned} d_{\max} &= \int_{t_0}^{t_1} \dot{d}\, d\tau = \int_{t_0}^{t_1} \left(\frac{\partial \overline{f}}{\partial \sigma_{ij}} \dot{\sigma}_{ij} - \dot{\sigma}_y \right) d\tau = \int_{t_0}^{t_1} \frac{\partial \overline{f}}{\partial \sigma_{ij}} \dot{\sigma}_{ij} d\tau \\ &= \sqrt{\frac{3}{2}} \dot{\sigma}_{ij} N_{ij} (t_1 - t_0). \end{aligned} \tag{95}$$

3.5 Smoothened saw tooth loading

The goal of this final example is to verify and summarize the analytical results obtained in the last 2 sections. We consider a smoothened version of the saw tooth loading that we used until now.The load function is represented on Fig. 24. It is a succession of linearly increasing loading and of constant loading

Since our main goal is to verify our analytic computations, the equivalent viscoplastic strain rate is the only quantity that shall be studied. The yield stress, the equivalent viscoplastic strain and the equivalent backstress can all be retrieved from $\dot{\overline{\varepsilon}}^{\text{vp}}$. On Fig. 25a the equivalent viscoplastic strain rate is represented for both an isotropic linear hardening model and a mixed linear hardening. Several values of the viscosity parameter η are represented. Fig. 25b is a zoom on the first half of the first cycle.

When the loading is constant, we observe that the equivalent viscoplastic strain rate follows a decreasing exponential. This is exactly what we predicted (see Eq. (71)). Our analytical results (see Eq. (84)) indicated that, during the loading stage, $\dot{\overline{\varepsilon}}^{\text{vp}}$ follows a law of the kind of $a\Big(1 - \exp(-t/b)\Big)$. This

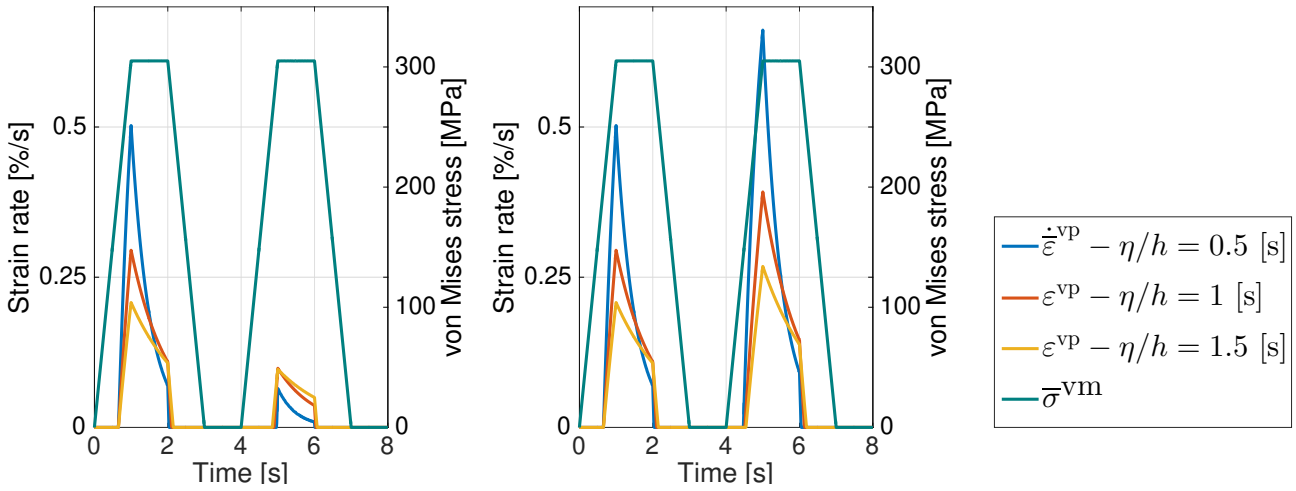

(a) Equivalent viscoplastic strain rate for 1 complete cycle

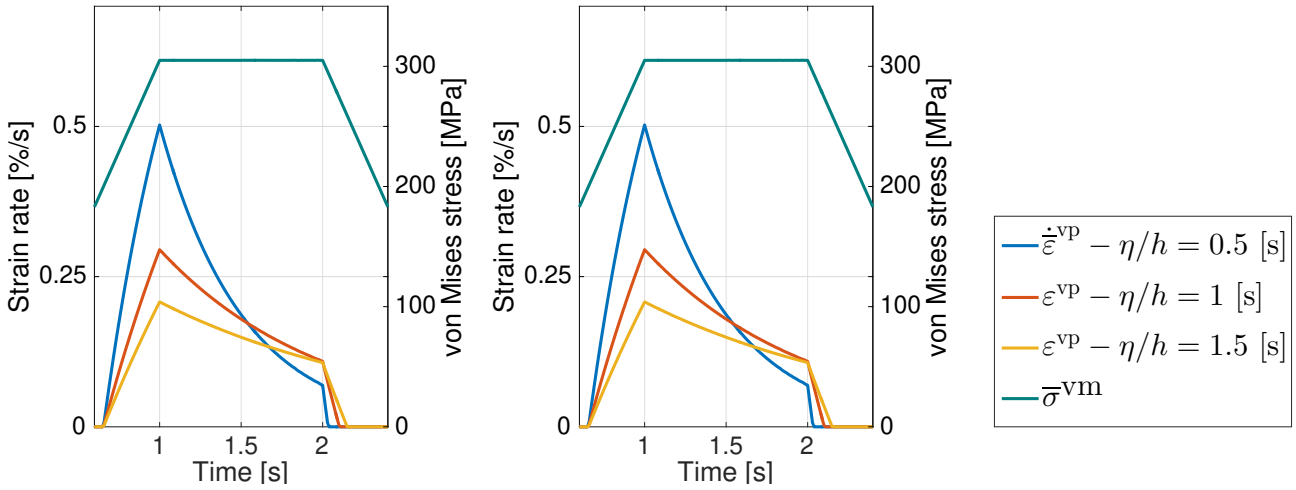

(b) Zoom on the first half of the first cycle

Fig. 25: Equivalent viscoplastic strain rate when the cube is subjected to smoothened loading/unloading cycle. Different values of η represented.

result is not contradicted by the simulations. For the unloading, we predicted a decreasing exponential. Using the results obtained by the simulations, we cannot verify it either.

4 Part 4: Sensitivity study of numerical parameters

In this section will be analysed the influence of some numerical parameters over the simulation. In a first time, a study over the loading speed, the spatial discretization and the temporal discretization will be performed. In a second time, one will determine the best suited parameters for each part of the study and verify if its possible to validate the numerical solution thanks to the total potential energy.

To analyse the influence over the numerical solution, one has to study the convergence of some parameters. The chosen ones are here the work of internal and external forces at the end of the simulation, and the yield stress σ_{Yield}. The choice to study the works done by the different forces is to verify if the total potential energy can validate the numerical solution. Indeed, if internal and external forces' works are equal, then the total potential energy is proved. The second choice of studying σ_{Yield} is because it is an important parameter to analyse in this project and thus its convergence is clearly important.

4.1 Loading speed

In this subsection, one will study the influence of the loading speed over the numerical simulation. By changing the parameter T_{cycle}, and by keeping the number of cycle of loading/unloading constant, it is possible to change the slope and then the loading speed of the simulation. Otherwise, the other parameters studied below are kept constant, to 1 for the number of element (spacial discretization) and to 0.1 for Δt (temporal discretization). The three types of model studied in this project will be analysed.

4.1.1 Elasto-plastic with linear hardening

From Section 1 will be in a first time studied the Elasto-plastic with linear hardening model. Two cases will be considered: a linear isotropic hardening and a linear mixed hardening.

1. **Linear isotropic hardening**

   On Fig. 26a below are represented the Internal and the external forces' works, for different T_{cycle}, as well as the absolute value of Total Potential Energy (TPE). A their own scales, the loading speed seems not influence that much the different works. On Fig. 26b is represented the yield stress. The look of the curves is the same except for a cycle time equal to 1 second. Otherwise, on Fig.27, one can observe that for a cycle time superior to 2 seconds, the curves almost overlap. It can be then conclude that for such a type of model, an ideal cycle time is superior to 2 seconds.

2. **Linear mixed hardening**

   The same observations as for the linear isotropic hardening model can be done. Indeed, the look of the curves on Fig. 26a and on Fig. 28a is the same. Otherwise, on Fig. 28b is again represented the yield stress. As for the linear isotropic hardening, the curve for a cycle time equal to 1 second is totally different than the other curves. A zoom over the first slopes of the curves has been done on Fig. 29. One can observe that again, the curves almost overlap for a cycle time superior to 2 seconds, as for a linear isotropic hardening.

That leads to the conclusion that for an elasto-plastic model with linear hardening, a good minimum value for the cycle time is 2 seconds.

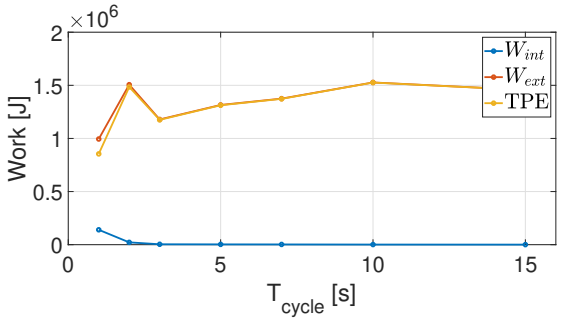

(a) Internal and external work in function of the cycle time for a linear isotropic hardening.

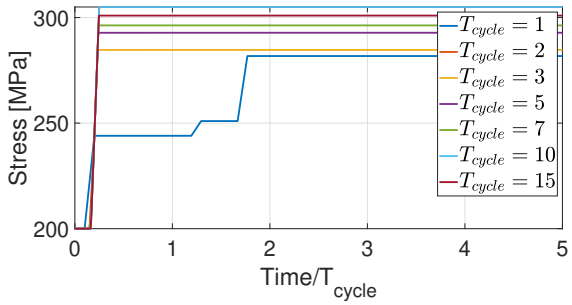

(b) Stress yield σ_{Yield} in function of the cycle time for a linear isotropic hardening.

Fig. 26: Influence of the loading speed over the internal and external work and over the stress yield for a linear isotropic hardening.

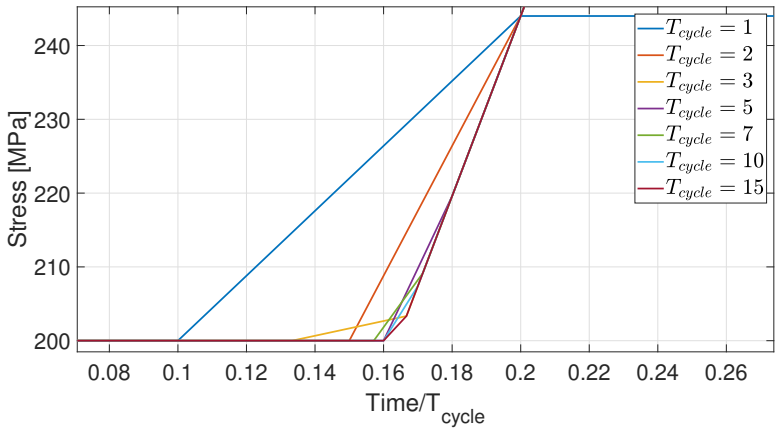

Fig. 27: Zoom over the Fig. 26b. Influence of the loading speed over the stress yield for a linear isotropic hardening.

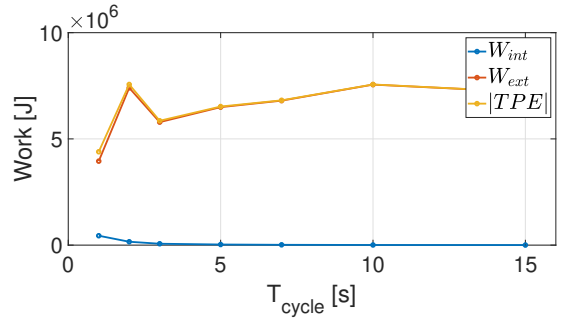

(a) Internal and external work in function of the cycle time for a linear isotropic hardening.

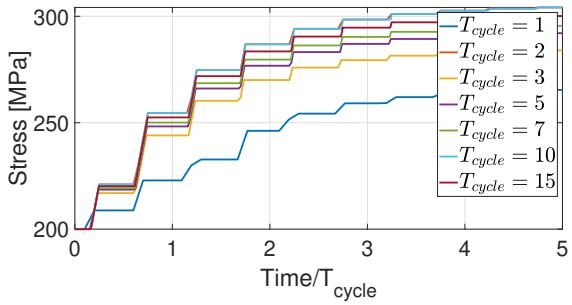

(b) Stress yield σ_{Yield} in function of the cycle time for a linear isotropic hardening.

Fig. 28: Influence of the loading speed over the internal and external work and over the stress yield for a linear isotropic hardening.

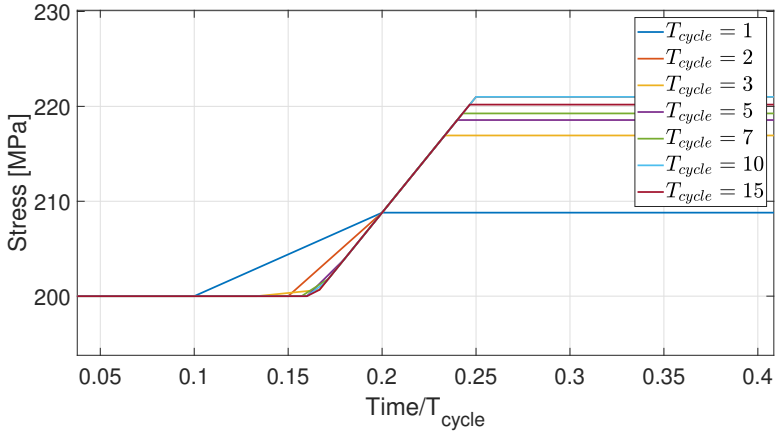

Fig. 29: Zoom over the Fig. 28b. Influence of the loading speed over the stress yield for a linear mixed hardening.

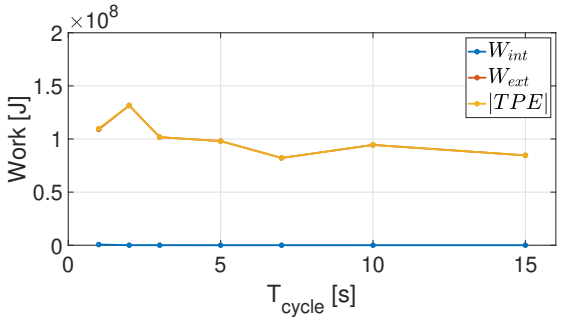

(a) Internal and external work in function of the cycle time for a non-linear kinematic hardening.

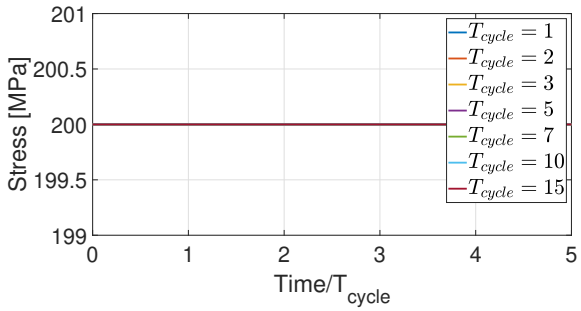

(b) Stress yield σ_{Yield} in function of the cycle time for a non-linear kinematic hardening.

Fig. 30: Influence of the loading speed over the internal and external work and over the stress yield for a non-linear kinematic hardening.

4.1.2 Elasto-plastic with non-linear hardening

Here will be studied two cases for an elasto-plastic model with non-linear hardening. The first case is about kinetic hardening only, and the second case is about mixed hardening.

1. **Non-linear kinetic hardening**

   On Fig. 30a, it can be observed that the cycle time seems have no so much influence over the works done by internal and external forces. It can be noticed that the absolute value of the TPE is maximized for a cycle time of 2 seconds. Otherwise, on Fig. 30b, one can be observed that the yield stress is constant. A priori, the loading speed has no influence over a elasto-plastic model with non-linear kinetic hardening.

2. **Non-linear mixed hardening**

   On Fig. 31a is represented again the different works of the system. The two curves of works, at their own scales, tend to be more or less constant, even if it can be observe a TPE maximal absolute value for a cycle time of 2 seconds. On Fig. 31b, the first slopes of the curves seem to overlap. By zooming on this area, as done on Fig. 32, the curves indeed overlap pretty well, even if it can be noticed that for a cycle time equals to 1 second, the curve moves away from the others.

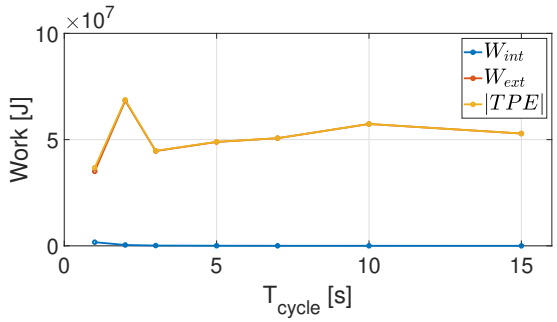

(a) Internal and external work in function of the cycle time for a non-linear mixed hardening.

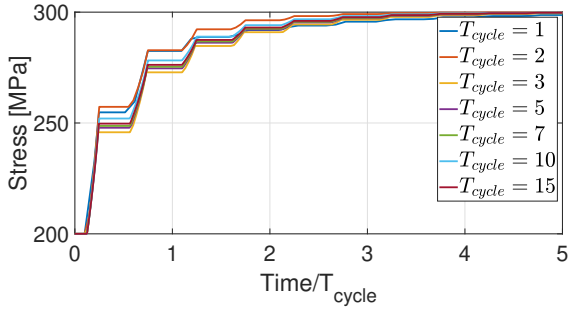

(b) Stress yield σ_{Yield} in function of the cycle time for a non-linear mixed hardening.

Fig. 31: Influence of the loading speed over the internal and external work and over the stress yield for a non-linear mixed hardening.

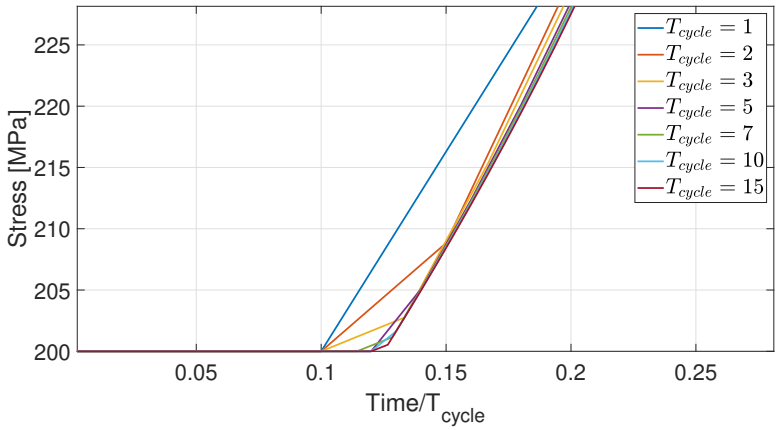

Fig. 32: Zoom over the Fig. 31b. Influence of the loading speed over the stress yield for a non-linear mixed hardening.

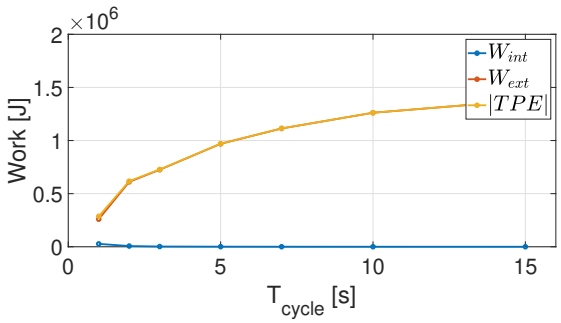

(a) Internal and external work in function of the cycle time for a elasto-viscoplastic model with linear isotropic hardening.

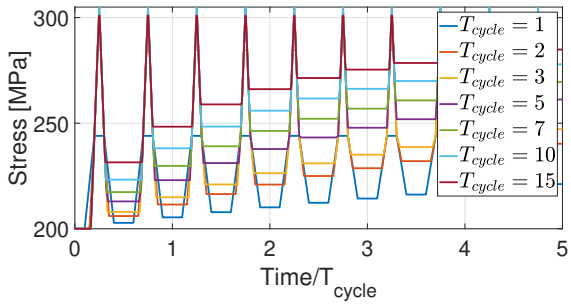

(b) Stress yield σ_{Yield} in function of the cycle time for a elasto-viscoplastic model with linear isotropic hardening.

Fig. 33: Influence of the loading speed over the internal and external work and over the stress yield for a elasto-viscoplastic model with linear isotropic hardening.

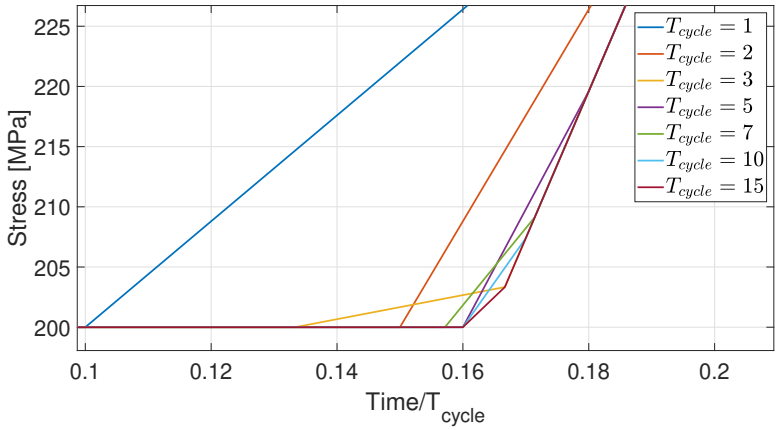

Fig. 34: Zoom over the Fig. 33b. Influence of the loading speed over the stress yield for a linear isotropic hardening (elasto-viscoplastic model).

For a elasto-plastic model with non-linear hardening, it can be then conclude that the cycle time seems not so important, even if it is maybe better to avoid a cycle time equals to 1 second, to be sure to have a convergence.

4.1.3 Elasto-viscoplastic with hardening

Like for the two previous subsections, a linear isotropic hardening and a linear mixed hardening will be studied for the elasto-viscoplastic model.

1. **With linear isotropic hardening**

   On the first Fig. 33a is represented the works of internal and external forces as well as the TPE at the end of the simulations for different cycle time. The work done by external forces is quite affected by this parameter. Otherwise, on Fig. 33b, the curves seem to overlap as far as the first slope is concerned. Moreover, this is confirmed by the Fig. 34, even if for a cycle time equals to 1 second, the curve is moving away a little.

2. **With linear mixed hardening**

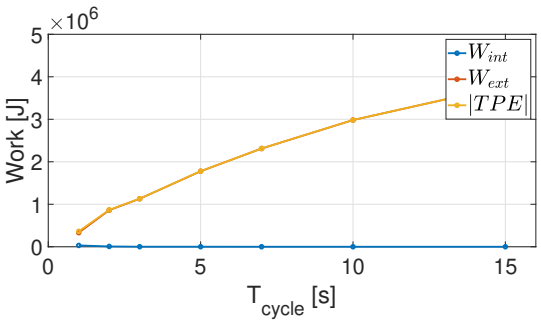

(a) Internal and external work in function of the cycle time for a elasto-viscoplastic model with linear mixed hardening.

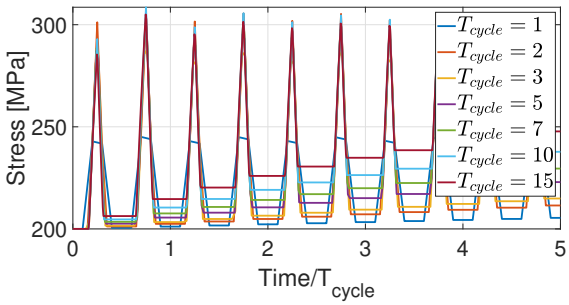

(b) Stress yield σ_{Yield} in function of the cycle time for a elasto-viscoplastic model with linear mixed hardening.

Fig. 35: Influence of the loading speed over the internal and external work and over the stress yield for a elasto-viscoplastic model with linear mixed hardening.

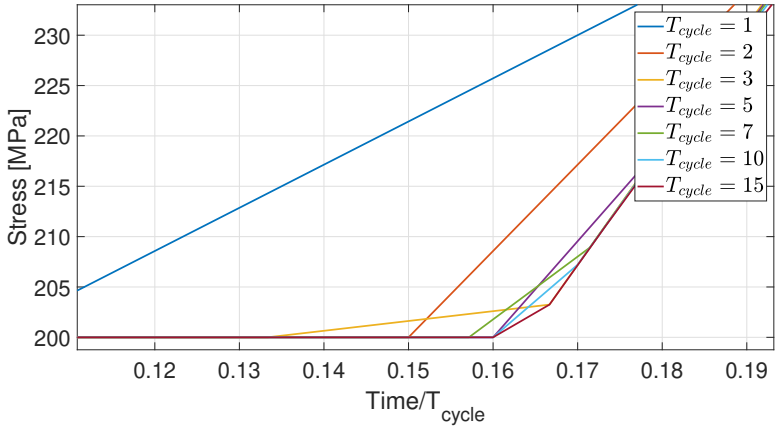

Fig. 36: Zoom over the Fig. 35b. Influence of the loading speed over the stress yield for a linear mixed hardening (elasto-viscoplastic model).

Here again, it can be seen on Fig. 35a that the TPE is minimal for a cycle time equals to 1 second, just as for an elasto-viscoplastic model with isotropic hardening. The same conclusion about the yield stress convergence can be done thanks to the Fig. 35b and 36, that is that the curves of stress yield nearly overlap, except for the cycle time equal to 1 second's curve.

It can be conclude that for an elasto-viscoplastic model with linear (isotropic or mixed) hardening, the best cycle time to satisfy the TPE is 1 second, even if it leads to a less better convergence of the yield stress.

4.2 Spatial discretization

In this subsection is studied the influence of the size of the mesh over the numerical simulation. The number of elements of the system is then changed, by keeping the same number of element for each direction. It has to be noticed that the maximum number of element per direction is here 6, because the Metafor Program accepts a maximum number of Node Set equal to 500.

4.2.1 Elasto-plastic with linear hardening

1. **Linear isotropic hardening**

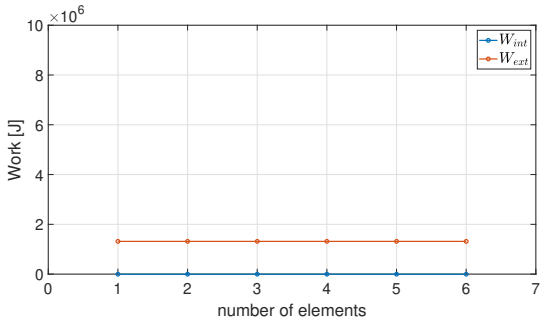

(a) Internal and external work in function of the number of elements for a linear isotropic hardening.

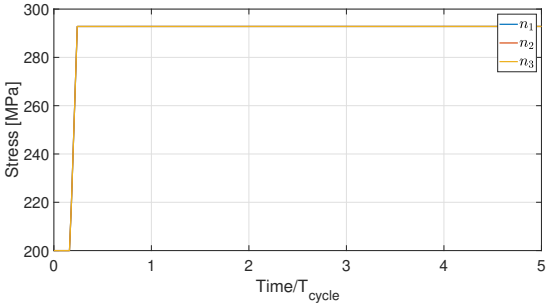

(b) Stress yield σ_{Yield} in function of the number of element for a linear isotropic hardening. n_1 corresponds to 1 element, n_2 to 2, and so on.

Fig. 37: Influence of spatial discretization over the internal and external work and over the stress yield for a linear isotropic hardening.

On Fig 37a, which represents the internal and external work, one can observe that it stays constant. They are equal to -2748.94 for the work of the internal forces and $1.31514e+06$ for the external forces' one. Those values are different, which means that the total potential energy theorem is not respected here yet, but with an other combination of parameters for the loading speed and for the time discretization, it could be possible. Otherwise, the number of elements seems not to be important here, because the works of internal and external forces stay constant, whatever the number of element.

On Fig. 37b, it is σ_{Yield} which is studied. It can be observed than, just as before, it converges for a number of elements superior to one[2]. It can be then conclude for the linear isotropic hardening that the number of elements isn't important.

2. **Linear mixed hardening**
   The same reasoning is made for the linear mixed hardening. For this case, the works of internal and external forces are respectively equal for any number of elements, as seen on Fig. 38a. Their values are $3.87284e+5$ for internal forces' work and $5.05809e+6$ for the external's. Moreover, one can observe that σ_{Yield} is also the same for every number of elements. One can then conclude than for a linear mixed hardening, the number of elements and so the mesh discretization do not influence the simulation.

This subsection about the spatial discretization of a linear hardening model makes then understand that the number of elements and so the mesh refinement does not influence the numerical solution.

4.2.2 Elasto-plastic with non-linear hardening

1. **Non-linear kinematic hardening**

   The same observations than the Elasto-plastic linear hardening can be done. The number of elements does not influence at all neither the works (see Fig. 39a), neither the yield stress (see Fig. 39b). Indeed, the values are the same for the works and the curves overlap perfectly for the yield stress.

2. **Non-linear mixed hardening**

[2]Note that the curves for n_1 and n_2 are hidden behind the curve for n_3

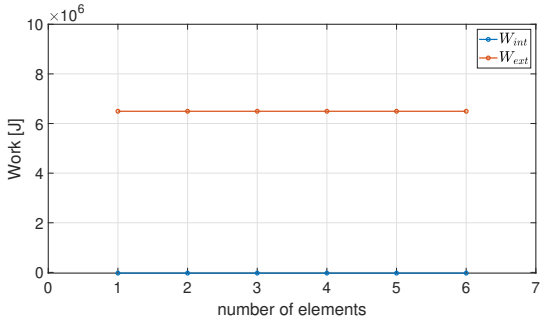

(a) Internal and external work in function of the number of elements for a linear mixed hardening.

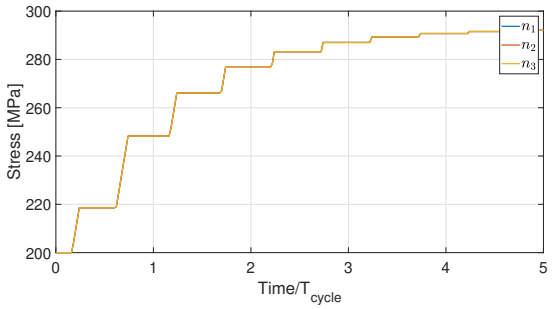

(b) Stress yield σ_{Yield} in function of the number of element for a linear mixed hardening. n_1 corresponds to 1 element, n_2 to 2, and so on.

Fig. 38: Influence of spatial discretization over the internal and external work and over the stress yield for a linear mixed hardening.

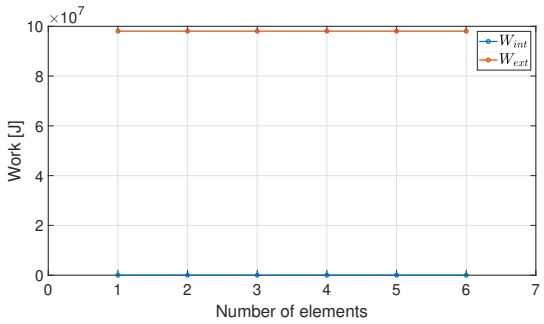

(a) Internal and external work in function of the number of elements for a non-linear kinematic hardening.

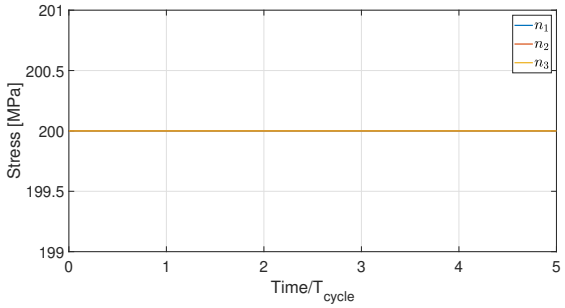

(b) Stress yield σ_{Yield} in function of the number of element for non-linear kinematic hardening. n_1 corresponds to 1 element, n_2 to 2, and so on.

Fig. 39: Influence of spatial discretization over the internal and external work and over the stress yield for a non-linear kinematic hardening.

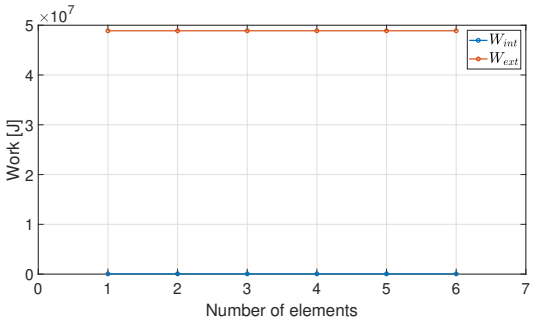

(a) Internal and external work in function of the number of elements for a non-linear mixed hardening.

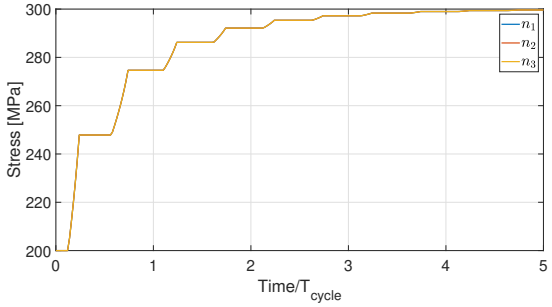

(b) Stress yield σ_{Yield} in function of the number of element for non-linear mixed hardening. n_1 corresponds to 1 element, n_2 to 2, and so on.

Fig. 40: Influence of spatial discretization over the internal and external work and over the stress yield for a non-linear mixed hardening.

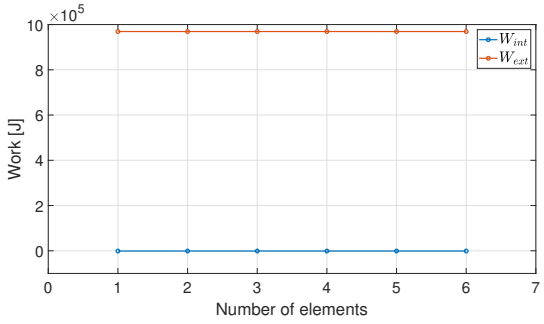

(a) Internal and external work in function of the number of elements for a elasto-viscoplastic model with linear isotropic hardening.

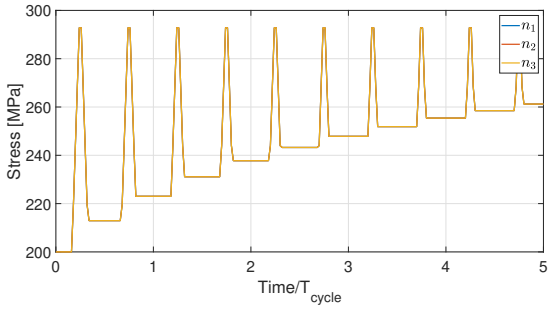

(b) Stress yield σ_{Yield} in function of the number of element for a elasto-viscoplastic model with linear isotropic hardening. n_1 corresponds to 1 element, n_2 to 2, and so on.

Fig. 41: Influence of spatial discretization over the internal and external work and over the stress yield for a elasto-viscoplastic model with linear isotropic hardening.

Once again, the spatial discretization seems to not influence the numerical solution, as seen on Fig. 40a and 40b. The values are exactly the same for the first graph and the curves overlap perfectly on the second.

4.2.3 Elasto-viscoplastic with hardening

1. **With linear isotropic hardening**
   One can see on the two figures Fig. 41a and Fig. 41b below that for any number of elements, the values of the variables studied stay constant. It can be then deduce that for a elasto-viscoplastic model, with linear isotropic hardening, the spatial discretization does not influence the numerical simulation. Moreover, once again, it can be noticed that the spacial discretization does not influence the works of internal and external forces. That implies that it doesn't affect the total potential energy, so the numerical simulation cannot be verify by modifying this parameter.

2. **With linear mixed hardening**
   The same observations as the elasto-viscoplastic model with linear isotropic hardening can be done. All values for the variables studied stay constant whatever the number of elements, as seen on Fig. 42a and 42b.

To conclude this section about spatial discretization, it has to be retained that the mesh and the

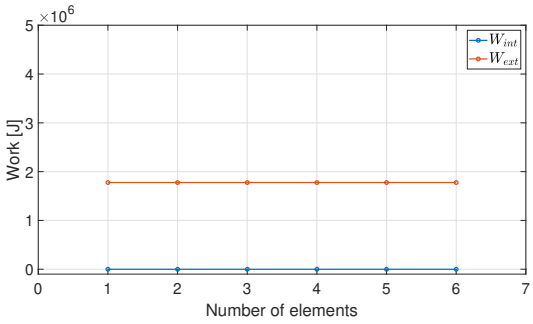

(a) Internal and external work in function of the number of elements for a elasto-viscoplastic model with linear mixed hardening.

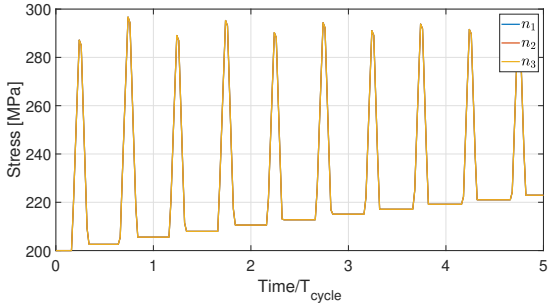

(b) Stress yield σ_{Yield} in function of the number of element for a elasto-viscoplastic model with linear isotropic hardening. n_1 corresponds to 1 element, n_2 to 2, and so on.

Fig. 42: Influence of spatial discretization over the internal and external work and over the stress yield for a elasto-viscoplastic model with linear mixed hardening.

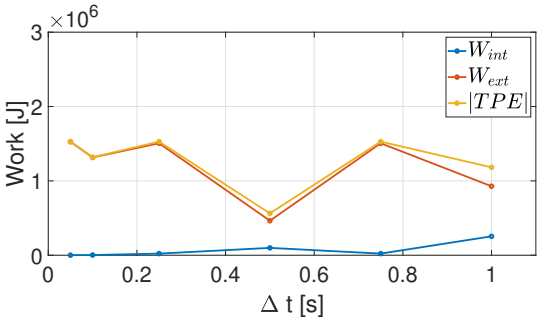

(a) Internal and external work in function of the time step for a linear isotropic hardening.

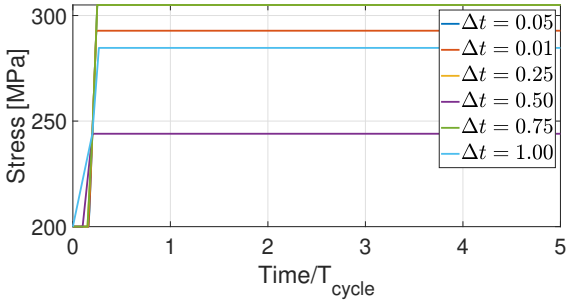

(b) Stress yield σ_{Yield} in function of the time step for a linear isotropic hardening.

Fig. 43: Influence of the temporal discretization over the internal and external work and over the stress yield for a linear isotropic hardening.

number of element have no influence on the numerical simulations.

4.3 Temporal discretization

In this subsection will be studied the influence of the time step over the numerical simulations. The other parameters are keeping constant, equals to 5 seconds for the cycle time and equals to 1 for the number of elements.

4.3.1 Elasto-plastic with linear hardening

As for the precedent analysis over numerical parameters, two cases will be studied for the elasto-plastic model with linear hardening: isotropic and mixed linear hardening.

1. **Linear isotropic hardening**

   The works of internal and external forces are represented on Fig. 43a. It seems that the absolute TPE maximal value is for a time step of 0.25 second. On Fig. 43b, the slopes of the yield stress nearly overlap, even if for a time step of 1 second, the slope's curve is a bit far.

2. **Linear mixed hardening**

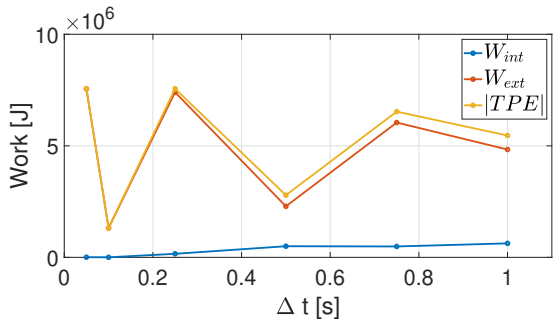

(a) Internal and external work in function of the time step for a linear mixed hardening.

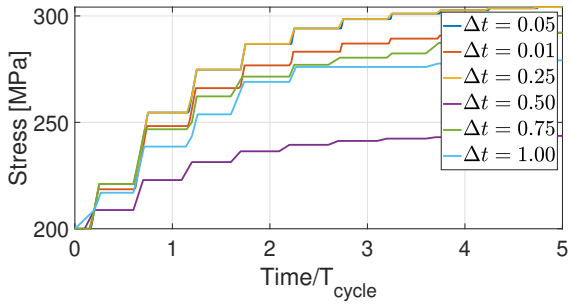

(b) Stress yield σ_{Yield} in function of the time step for a linear mixed hardening.

Fig. 44: Influence of the temporal discretization over the internal and external work and over the stress yield for a linear mixed hardening.

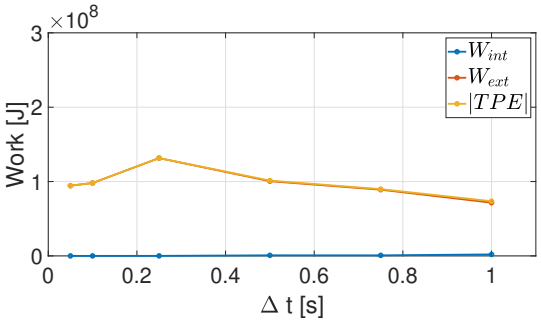

(a) Internal and external work in function of the time step for a non-linear kinematic hardening.

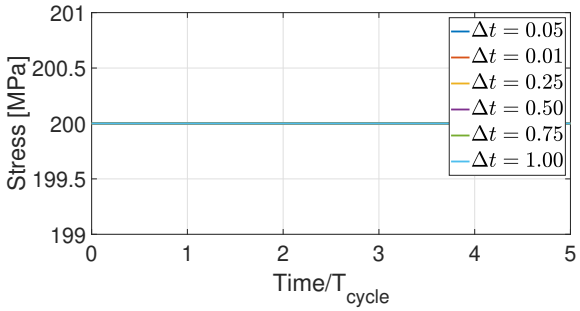

(b) Stress yield σ_{Yield} in function of the time step for a non-linear kinematic hardening.

Fig. 45: Influence of the temporal discretization over the internal and external work and over the stress yield for a non-linear kinematic hardening.

On Fig. 44a is represented once again the works for internal and external forces. The absolute value of the TPE seems maximal for a time step of 0.25 second. On Fig. 44b, as for the linear isotropic hardening, the first slopes of the curves are close.

For an elasto-plastic model with linear hardening, it seems that the best time step could be 0.25 in regards to maximize the absolute value of the TPE.

4.3.2 Elasto-plastic with non-linear hardening

1. **Non-linear kinematic hardening**

   For non-linear kinematic hardening, the yield stress represents on Fig. 45b is always constant, whatever the time step. It is then difficult to analyse a possible convergence with this variable. Otherwise, on Fig. 45a, it seems that the best time step is 0.25 second. It will surely be possible to confirmed this supposition with the results of the non-linear mixed hardening.

2. **Non-linear mixed hardening**

   The maximal TPE on Fig. 46a is for a time step of 0.25 second. Otherwise, on Fig. 46b, it seems that the first slope of the curve for a time step equals to 1 second does not overlap the other curves, but that for lower time steps, they overlap well.

It can be then conclude that for a non-linear hardening, the best time step is 0.25 second.

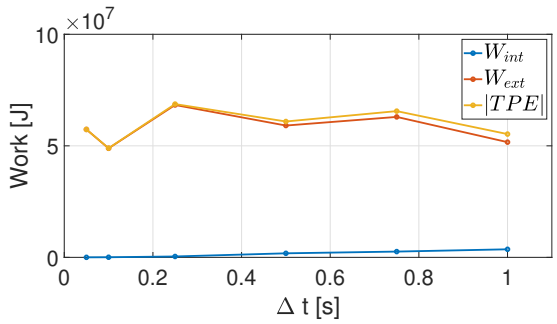

(a) Internal and external work in function of the time step for a non-linear mixed hardening.

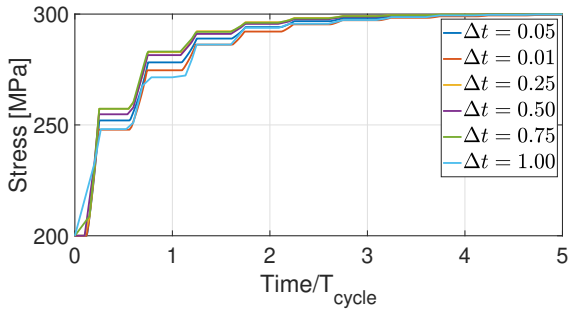

(b) Stress yield σ_{Yield} in function of the time step for a non-linear mixed hardening.

Fig. 46: Influence of the temporal discretization over the internal and external work and over the stress yield for a non-linear mixed hardening.

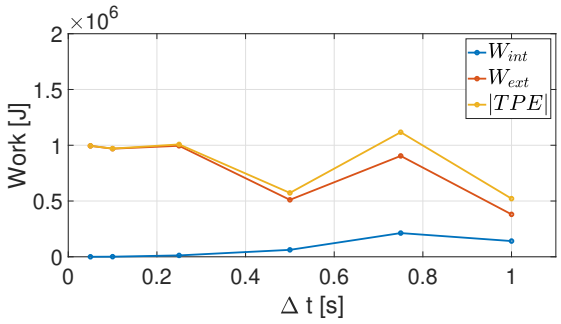

(a) Internal and external work in function of the time step for a elasto-viscoplastic model with linear isotropic hardening.

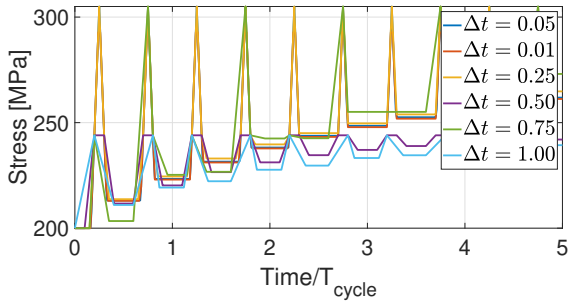

(b) Stress yield σ_{Yield} in function of the time step for a elasto-viscoplastic model with linear isotropic hardening.

Fig. 47: Influence of the temporal discretization over the internal and external work and over the stress yield for a elasto-viscoplastic model with linear isotropic hardening.

4.3.3 Elasto-viscoplastic with hardening

1. **With linear isotropic hardening**

   On Fig. 47a, the time step that maximized the better the total potential energy is 0.25 or 0.75 second. Furthermore, on Fig. 47b, it seems that the curve of the time step equals to 0.75 second converges less towards others. It can be then conclude here that for an elasto-viscoplastic model with linear isotropic hardening, the time step of 0.25 second is the best.

2. **With linear mixed hardening**

   The same conclusion than for the isotropic hardening can be done here by observing the Fig. 48a and Fig. 48b. The best time step for this kind of model is then 0.25 second.

4.4 Conclusion about the study of the numerical parameters

The best numerical parameters for each model are resumed in the Table 1, 2 and 3 here below. The TPE is calculated for each model too, from the works of internal and external forces at the end of the simulations. The results below are every time for a mixed hardening.

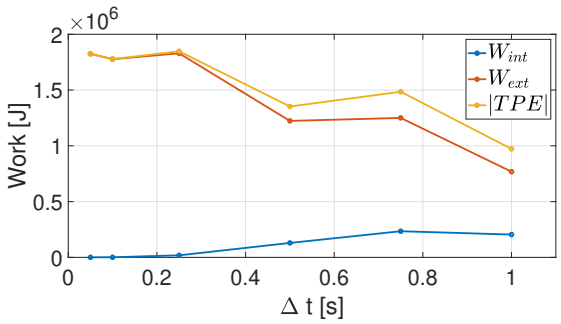

(a) Internal and external work in function of the time step for a elasto-viscoplastic model with linear mixed hardening.

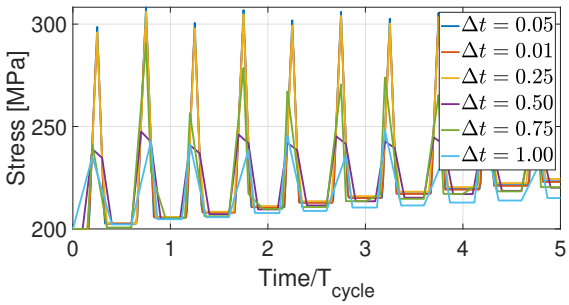

(b) Yield stress σ_{Yield} in function of the time step for a elasto-viscoplastic model with linear mixed hardening.

Fig. 48: Influence of the temporal discretization over the internal and external work and over the stress yield for a elasto-viscoplastic model with linear mixed hardening.

Cycle time	2 seconds
Number of elements	1 (doesn't affect)
Time step	0.25 second
W_{int}	1.37585e+06 J
W_{ext}	1.4436e+07 J
W_{TPE}	1.581185e+07 J

Table 1: Best numerical parameters for a elasto-plastic model with linear hardening and results of works done by internal and external forces for numerical simulations with those parameters.

It is important to mention that, no matter the model studied, the spatial discretization does not affect the numerical simulation. It can be explain by the fact that stress and strain stay constant inside the cube. The loading speed seems affect the simulations, but not that much. It is mostly for the research of a maximal absolute value of the TPE that it will be determined. Finally, it is the time step that influences the most the numerical simulations, as seen in the previous section.

The different absolute value of the TPE calculated here are quietly higher than the values seen on the different previous Figures. The goal was to maximize it to validate the that numerical simulations approach the real comportment of the material. Then, it can be affirm here that the TPE theorem validate the numerical scheme used in our project.

Cycle time	2 seconds (doesn't affect)
Number of elements	1 (doesn't affect)
Time step	0.25 second
W_{int}	3.25631e+06 J
W_{ext}	5.88012e+07 J
W_{TPE}	6.205751e+07 J

Table 2: Best numerical parameters for a elasto-plastic model with non-linear hardening and results of works done by internal and external forces for numerical simulations with those parameters.

Cycle time	2 second
Number of elements	1 (doesn't affect)
Time step	0.25 second
W_{int}	41386.5 J
W_{ext}	2.55636e+06 J
W_{TPE}	2.5977465e+06 J

Table 3: Best numerical parameters for a elasto-viscoplastic model with linear hardening and results of works done by internal and external forces for numerical simulations with those parameters.

Conclusion

In Part 1, we studied various linear hardening models in both a state of plane stress and plane strain. The studied models were the elastic perfectly plastic model, the linear isotropic hardening, the linear kinematic hardening and the linear mixed hardening. The elastic perfectly plastic model fails as soon as the von Mises stress become larger than the yield stress. The linear isotropic model cannot account for the Bauschinger effect. The linear kinematic hardening can represent the Bauschinger effect quite well. However it leads ineluctably to ratchetting which causes the failure of the material. Because it combines the isotropic and the kinematic hardening, the mixed linear hardening can better represent real-world materials and leads to a more realistic elasto-plastic behavior. We observed that during a tensile test the three hardening models have the same behavior. This translates itself into the fact that the equivalent plastic strain is the same no matter the linear hardening model considered.

All these models were studied in the case of a loading/unloading cycle: the applied load goes from zero to t_{max} then from t_{max} to $-t_{\text{max}}$ and finally back to zero. This loading/unloading cycle starts by putting the cube in traction then in compression. We inversed this order to investigate its effects. It has a big impact in the case of the linear isotropic model. The cube will stay deformed in the same way as it was deformed for the first time. If it was first put in compression, it will remain compressed even after an infinite amount of loading/unloading cycles. In the case of the kinematic and mixed linear hardening, the order has no direct impact. What odes matter is when the load stops to be applied. If the cube was last put in compression, there will remain an anisotropy. The cube will deform more easily in compression than in traction.

Still while studying linear hardening models, we demonstrated analytically that the plastic dissipation evolves linearly with the loading/time. This results is independent of the model considered. However this doesn't mean that the same amount of energy is dissipated by each model. Each model doesn't spend the same amount of time in the plastic region.

Part 2...

In Part 3, the elasto-viscoplastic behavior of the cube was studied using Perzyna's law to model the viscosity. Linear isotropic and linear kinematic hardening laws were used to model the plasticity. We found that the ratio η/h which has the units of a time is the characteristic time of the static response of the material. We demonstrated that during a constant loading the equivalent viscoplastic strain converges towards a finite value and that this convergence follows an exponential. When investigating loading/unloading at constant rate, we discovered the viscosity dominated regime. The condition to lies in this regime is that the viscosity parameter divided by the hardening constant h must be much larger than the characteristic period of time during which the cube lies in the viscoplastic region.

Afterwards, still while investigating the elasto-viscoplasticity, we studied the distance to the yield surface with respect ot the yield center $d = \overline{\sigma}^{\text{VM}} - \sigma_y$. It may also be called the overstress because it characterizes how much larger is the von Mises stress with respect to the yield stress. We found an analytical expression. From this expression, we deduced the maximal overstress d_{max} during a loading/unloading stage. We simplified this expression in the case of the viscosity dominated regime and concluded that d_{max} is independent of the loading speed in the framework of this regime. Lastly, we verified our theoretical predictions by simulating a smoothened saw tooth loading.

Finally, in Part 4, the numerical parameters T_{cycle} for the loading speed, the number of elements for the spatial discretization, and the time step for the temporal discretization have been studied. The results show that the spatial discretization has absolutely no influence over the numerical simulation. The loading speed has a little influence, but the parameter that change everything is the time step. For each type of model, the best parameters are 2 seconds for the cycle time and 0.25 second for the time step. Once again, the number of elements does not matter. Thanks to those parameters, it has been possible to determine the maximum values of the absolute values of the TPE for the best numerical parameters.

References

[1] Ponthot, J.-P. (2020). *Advanced Solid Mechanics*. University of Liège.

[2] Kelly, P. (2020). Solid Mechanics Part II: Engineering Solid Mechanics – small strain. Solid mechanics lecture notes, University of Auckland.